Geomechanics and Engineering, *Vol. 32, No. 2 (2023) 159-177*
https://doi.org/10.12989/gae.2023.32.2.159

Visco-elastic foundation effect on buckling response of exponentially graded sandwich plates under various boundary conditions

Mimoun Bennedjadi[1], Salem Mohammed Aldosari[2,3a], Abdelbaki Chikh*[1,4], Abdelhakim Kaci[1,5], Abdelmoumen Anis Bousahla[6], Fouad Bourada[1,7], Abdeldjebbar Tounsi[8], Kouider Halim Benrahou[1,9] and Abdelouahed Tounsi[1,10,11]

[1]*Material and Hydrology Laboratory, University of Sidi Bel Abbes, Faculty of Technology, Civil Engineering Department, Algeria*
[2]*Enhanced Composite and Structures Centre, School of Aerospace, Transport, and Manufacturing, Cranfield University, Cranfield MK43 0AL, UK*
[3]*National Center for Aviation Technology, King Abdulaziz City for Science and Technology (KACST), Riyadh 11442, Saudi Arabia*
[4]*Ibn Khaldoun University, BP 78 Zaaroura, 14000 Tiaret, Algeria*
[5]*Université Dr. Tahar Moulay, Faculté de Technologie, Département de Génie Civil et Hydraulique, BP 138 Cité En-Nasr 20000 Saida, Algérie*
[6]*Laboratoire de Modélisation et Simulation Multi-échelle, Université de Sidi Bel Abbés, Algeria*
[7]*Département des Sciences et de la Technologie, université de Tissemsilt, BP 38004 Ben Hamouda, Algérie*
[8]*Industrial Engineering and Sustainable Development Laboratory, University of Rélizane, Faculty of Science & Technology, Mechanical Engineering Department, Algeria*
[9]*Department of Physics, College of Sciences, Princess Nourah bint Abdulrahman University (PNU), P.O. Box 84428, Riyadh 11671, Saudi Arabia*
[10]*YFL (Yonsei Frontier Lab), Yonsei University, Seoul, Korea*
[11]*Department of Civil and Environmental Engineering, King Fahd University of Petroleum &Minerals, 31261 Dhahran, Eastern Province, Saudi Arabia*

(*Received April 21, 2021, Revised October 18, 2022, Accepted January 3, 2023*)

Abstract. In the present work, a simple and refined shear deformation theory is used to analyze the effect of visco-elastic foundation on the buckling response of exponentially-gradient sandwich plates under various boundary conditions. The proposed theory includes indeterminate integral variables kinematic with only four generalized parameters, in which no shear correction factor is used. The visco-Pasternak's foundation is taken into account by adding the influence of damping to the usual foundation model which characterized by the linear Winkler's modulus and Pasternak's foundation modulus. The four governing equations for FGM sandwich plates are derived by employing principle of virtual work. To solve the buckling problem, Galerkin's approach is utilized for FGM sandwich plates for various boundary conditions. The analytical solutions for critical buckling loads of several types of powerly graded sandwich plates resting on visco-Pasternak foundations under various boundary conditions are presented. Some numerical results are presented to indicate the effects of inhomogeneity parameter, elastic foundation type, and damping coefficient of the foundation, on the critical buckling loads.

Keywords: buckling; functionally graded materials; Galerkin's approach; refined shear deformation theory; sandwich plates; various boundary conditions; visco-Pasternak foundations

1. Introduction

Functionally graded materials (FGMs) have received considerable attention in many engineering applications such as automotive, aerospace, civil and mechanical engineering structures (Karami and Janghorban 2020, Shahmohammadi *et al.* 2020, Sadoughifar *et al.* 2020, Abdelrahman 2020, Bouiadjra et al.2020, Arefi and Zur 2020, Dehsaraji *et al.* 2020, Feng *et al.* 2020) since they were first reported in 1980s (Yamanoushi *et al.* 1990, Koizumi 1993) FGMs are heterogeneous materials in which the material properties are varied continuously from point to point and thus eliminate the stress concentration encountered in laminated composites.

This is achieved by varying the volume fraction of the constituents, for example, of ceramic and metal in a predetermined manner. FGMs are now developed for general use as structural elements in different applications (Wang and Shen 2013, Akgöz and Civalek 2013, Shen and Yang 2014, Akbaş 2015, Daouadji *et al.* 2015, Li and Yang 2016, Attia 2017, Panjehpour *et al.* 2018, Ahmed *et al.* 2019, Avcar 2019, Ramteke *et al.* 2019, Madenci 2019, 2021, Asiri *et al.* 2020, Hadji 2020, Vinyas 2020, Trabelsi *et al.* 2020, Naz *et al.* 2020, Selmi 2020, Eltaherand Akbaş 2020, Li *et al.* 2021, Kertész *et al.* 2020, Alnujaie *et al.* 2021, Bashiri *et al.* 2021, Vinh 2021, Li and Zhang 2021, Tran and Cuong-Le 2022, Cuong-Le *et al.* 2022a, b).

Several theories are available in the literature for analyzing buckling response of functionally graded (FG)

*Corresponding author, Professor
E-mail: cheikhabdelbakki@yahoo.fr
[a]Professor
E-mail: saldosari@kacst.edu.sa

ISSN: 2005-307X (Print), 2092-6219 (Online)

sandwich plates resting on visco-Pasternak foundations. The simplest theory is called classical plate theory (CPT)

which is based on the Kirchhoff hypothesis. This theory ignores the transverse shear strain and it is only acceptable for thin plates (Zhang 2001, Ghannadpour *et al.* 2013, Wang *et al.* 2016, Wang and Zu 2017).For surmounts this problem, the first order shear deformation theory (FSDTs) have been developed by assumption that the in-plane displacements are linearly distributed across the plate thickness. This leads to the transverse shear stresses being constant across the plate thickness, so the zero shear stress condition on the plate face is not satisfied (Reissner 1944, Reissner 1945, Mindlin 1951). However, virtually an appropriate shear correction factor is needed. In order to include the curvature of the normal after deformation, a number of theories known as higher–order shear deformation theories (HSDT) have been devised in which the displacements are assumed quadratic or cubic through the thickness of the plate.The higher order shear deformation plate theory (HSDT) satisfies zero shear stress conditions at top and bottom surfaces of plates. A shear correction factor is, therefore, not required (Ghasemabadian and Kadkhodayan 2016, Sobhy and Zenkour 2018, Zenkour 2018, Navale and Pise 2021, Onyeka and Edozie 2021).

Sandwich plates have received considerable attention in many engineering applications. Sandwich structures of material with gradients of properties (FG) have been proposed in which the core or two skins can be made from materials with gradient properties (FGM) because of remarkable advantages of the FGM. Many research papers have been developed to analyses FGM and composite sandwich structures (Anderson 2003, Bhangale and Ganesan 2006, Shodja *et al.* 2007, Etemadi *et al.* 2009, Zouatnia and Hadji 2019, Bharath *et al.* 2020, Rahmani *et al.* 2020, Katariya and Panda 2020, Hadji and Avcar 2021). Recently, a number of analytical and numerical analyzes were performed to study the mechanical response of the FG plate resting on foundations. To describe the interaction between the plate and the medium elastic, different types of elastic medium models have been proposed. The most simple is the one-parameter Winkler model (Winkler 1867) which models the midpoint elastic in the form of a series of tightly vertical linear elastic springs spaced and mutually independent. A more realistic and generalized representation of elastic medium can be achieved by means of a two elastic medium model settings. One of these physical models is the elastic model of the Pasternak type (Pasternak 1954). The first parameter of the Pasternak model represents the normal pressure then that the second parameter takes into account the transverse shear stress due to the interaction of the shear strain of the surrounding elastic medium. The composite and FG plates resting on foundations have wide applications in modern engineering and are widely used to investigate the mechanical behaviors of various structures (Tj *et al.* 2006, Huang *et al.* 2008, Yaghoobi and Yaghoobi 2013, Tornabene *et al.* 2014, Kim 2015, Allahkarami *et al.* 2016, Nebab *et al.* 2019, 2020, Rachedi *et al.* 2020, Merzoug *et al.* 2020, Kunbar *et al.* 2020, Boulal *et al.* 2020, Timesli 2020, Sobamowo 2020, Chami *et al.* 2020, Balubaid *et al.* 2021). Some research papers have investigated the mechanical response of the FG plate based on visco-elastic foundation (Fan *et al.* 2018, Hosseini *et al.* 2016, Zamani *et al.* 2017, Ebrahimi and Barati2016).Other works have been studied experimentally and numerically taking into account the effects of the interaction by considering other types of materials and other models (Yaylacı *et al.* 2020a, b, Yaylaci 2016, Yaylaci and Birinci 2013, Oner et al.2015, Adiyaman *et al.* 2015, Yaylacı *et al.* 2021a, b, c, d). Many researchers have been interested in methods for optimizing composite structures, which is generally more difficult, which aims to increase the accuracy of the results and to shorten the optimization time. Khatir *et al.* (2021) proposed the improved artificial neural network using arithmetic optimization algorithm (IANN-AOA) to address the damage quantification problem in functional gradient material (FGM) plate structures. Zenzen *et al.* (2020) used a two-step approach focusing on a modified transmissibility damage indicator and ANN to estimate the location and size of damage in composite structures. Khatir *et al.* (2019) presented a structural damage assessment technique using vibration data to identify damage. Cuong-Le *et al.* (2020a) presented a three-dimensional (3D) solution for free vibration and buckling analysis of FGM porous annular plate, conical, cylindrical and cylindrical shell using isogeometric analysis (IGA). Saadatmorad *et al.* (2021) used a new method called wavelet transform-based convolutional neural network (WT-CNN) technique to detect the location of damage in rectangular laminated composite plates. To obtain the deflection of the plate, the Reddy higher-order plate theory coupled with isogeometric analysis (IGA) is utilized by Cuong-Le *et al.* (2020b). Shahmohammadi *et al.* (2020) presented a Finite strip method for stability and free vibration analysis of sandwich functionally graded and laminated composite shells

In this article, visco-elastic foundation effect on buckling response of exponentially graded sandwich plates under various boundary conditions by using a simply refined shear deformation theory is presented. The proposed theories contain only four unknowns and satisfy the equilibrium conditions at the upper and lower surfaces of the plate without the use of shear correction factors. The displacement field of the proposed theory is chosen as a function of the nonlinear variation of displacements in the plane through the thickness. There are two major contributions: the use of an exponential plate theory with only four generalized parameters, and the investigation on the effect of boundary conditions on the buckling load of FG sandwich plates resting on visco-elastic foundation. Different types of FGM sandwich structures are taken. The visco-Pasternak's foundation is taken into account by adding the impact of damping to the usual foundation model which characterized by the linear Winkler's modulus and Pasternak's foundation modulus. The analytical equations of the plate are obtained using Galerkin's method for different boundary conditions. The accuracy of the solutions obtained is verified by comparing the current results with those predicted by the solutions available in the literature.

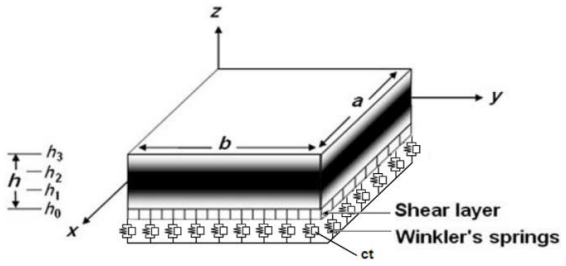

Fig. 1 Geometry of the EGM sandwich plate resting on Visco-elastic foundations

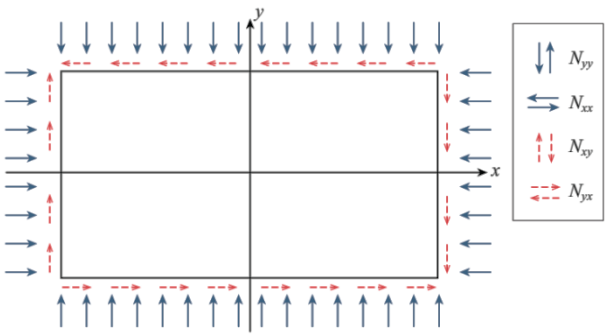

Fig. 2 Rectangular plate subjected to in-plane forces (Neves *et al*. 2012)

2. Theoretical formulation

2.1 Modeling of functionally graded material

Consider a composite structure made of three isotropic layers of arbitrary thickness h, length a and width b. The FGM sandwich plate is supported at four edges defined in the (x,y,z) coordinate system with x- and y-axes located in the middle plane ($z = 0$) and its origin placed at the corner of the plate. The vertical positions of the two interfaces between the core and faces layers are denoted, respectively, by $h_1$and h_2. The sandwich core is a ceramic material and skins are composed of a functionally graded material across the thickness direction. The bottom skin varies from a metal-rich surface $(z = h_0 = -h/2)$ to a ceramic-rich surface while the top skin face varies from a ceramic-rich surface to a metal-rich surface $(z = h_3 = h/2)$. It is assumed to be rested on a visco-Pasternak foundation model with k_w represents the Winkler stiffness, while c_t and k_s viscosityparameter and the shear layer foundation stiffness, respectivelyas illustrated in Fig. 1. The volume fraction of the ceramic phase is obtained from a simple rule of mixtures as

$$\begin{aligned} V^{(1)} &= \left(\frac{z-h_0}{h_1-h_0}\right)^k, && z\in[h_0,h_1] \\ V^{(2)} &= 1, && z\in[h_1,h_2] \\ V^{(3)} &= \left(\frac{z-h_3}{h_2-h_3}\right)^k, && z\in[h_2,h_3] \end{aligned} \tag{1}$$

where $V^{(n)}$, *(n =1, 2, 3)*, denotes the volume fraction functi on of layer n; k is the volume fraction index $(0 \le k \le +\infty)$, which dictates the material variation profile throug h the thickness. Note that the core of the present sandwich a nd any isotropic material can be obtained as a particular cas e of the power-law function by setting $p = 0$. The volume f raction for the metal phase is given as $V_m = 1 - V_c$.

The mechanical properties of functionally graded materials are often being represented in the exponentially graded form and power law variations one (Sobhy 2013). Based on an exponential law distribution, the material properties $P^{(n)}(z)$ of the E-FGM, such as Young's modulus E, are determined as

$$P^{(n)}(z) = P_m \exp\left(\beta V^{(n)}\right), \quad \beta = \ln\left(E_c/E_m\right), \quad (n = 1,2,3) \tag{2}$$

Poisson's ratio ν is assumed to be a constant value through the sandwich plate thickness.

The sandwich plate is subjected to compressive in-plane forces acting on the mid-plane of the plate. $\overline{N}_{xx}$ and $\overline{N}_{yy}$ denote the in-plane loads perpendicular to the edges $x = 0$ and $y = 0$ respectively, and $\overline{N}_{xy}$ denotes the distributed shear force parallel to the edges $x = 0$ and $y = 0$ respectively (see Fig. 2).

2.2 A new four-unknown shear deformation theory

2.2.1 Kinematics and constitutive equations

In this study, further simplifying supposition are made to the conventional HSDT so that the number of unknowns is reduced. The displacement field of the conventional HSDT is given by

$$\begin{aligned} u(x,y,z,t) &= u_0(x,y,t) - z\frac{\partial w_0}{\partial x} + f(z)\phi_x(x,y,t) \\ v(x,y,z,t) &= v_0(x,y,t) - z\frac{\partial w_0}{\partial y} + f(z)\phi_y(x,y,t) \\ w(x,y,z,t) &= w_0(x,y,t) \end{aligned} \tag{3}$$

$u_0, v_0, w_0, \phi_x, \phi_y$ are the five unknown displacement of the mid-plane of the plate. By considering that $\phi_x = k_1\int\theta(x,y,t)\,dx$ and $\phi_y = k_2\int\theta(x,y,t)\,dy$ (Mantari and Granados 2015a, b). In this article, the conventional HSDT is modified by proposing some simplifying suppositions so that the number of unknowns is reduced as

$$\begin{aligned} u(x,y,z,t) &= u_0(x,y,t) - z\frac{\partial w_0}{\partial x} + k_1 f(z)\int\theta(x,y,t)\,dx \\ v(x,y,z,t) &= v_0(x,y,t) - z\frac{\partial w_0}{\partial y} + k_2 f(z)\int\theta(x,y,t)\,dy \\ w(x,y,z,t) &= w_0(x,y,t) \end{aligned} \tag{4}$$

The constants k_1 and k_2 depends on the geometry. The shape functions $f(z)$ are chosen to satisfy the stress-free boundary conditions on the top and bottom surfaces of the plate, thus a shear correction factor is not required. In this study, the shape function is considered.

$$f(z) = \frac{z\left(\pi + 2\cos\left(\frac{\pi z}{h}\right)\right)}{(2+\pi)} \tag{5}$$

The nonzero linear strains are

$$\begin{Bmatrix}\varepsilon_x\\ \varepsilon_y\\ \gamma_{xy}\end{Bmatrix}=\begin{Bmatrix}\varepsilon_x^0\\ \varepsilon_y^0\\ \gamma_{xy}^0\end{Bmatrix}+z\begin{Bmatrix}k_x^b\\ k_y^b\\ k_{xy}^b\end{Bmatrix}+f(z)\begin{Bmatrix}k_x^s\\ k_y^s\\ k_{xy}^s\end{Bmatrix},\quad \begin{Bmatrix}\gamma_{yz}\\ \gamma_{xz}\end{Bmatrix}=g(z)\begin{Bmatrix}\gamma_{yz}^0\\ \gamma_{xz}^0\end{Bmatrix} \quad (6)$$

where

$$\begin{Bmatrix}\varepsilon_x^0\\ \varepsilon_y^0\\ \gamma_{xy}^0\end{Bmatrix}=\begin{Bmatrix}\dfrac{\partial u_0}{\partial x}\\ \dfrac{\partial v_0}{\partial y}\\ \dfrac{\partial u_0}{\partial y}+\dfrac{\partial v_0}{\partial x}\end{Bmatrix},\quad \begin{Bmatrix}k_x^b\\ k_y^b\\ k_{xy}^b\end{Bmatrix}=\begin{Bmatrix}-\dfrac{\partial^2 w_0}{\partial x^2}\\ -\dfrac{\partial^2 w_0}{\partial y^2}\\ -2\dfrac{\partial^2 w_0}{\partial x\partial y}\end{Bmatrix}, \quad (7a)$$

$$\begin{Bmatrix}k_x^s\\ k_y^s\\ k_{xy}^s\end{Bmatrix}=\begin{Bmatrix}k_1\theta\\ k_2\theta\\ k_1\dfrac{\partial}{\partial y}\int\theta\,dx+k_2\dfrac{\partial}{\partial x}\int\theta\,dy\end{Bmatrix},\quad \begin{Bmatrix}\gamma_{yz}^0\\ \gamma_{xz}^0\end{Bmatrix}=\begin{Bmatrix}k_2\int\theta\,dy\\ k_1\int\theta\,dx\end{Bmatrix} \quad (7b)$$

and $g(z)$ is given as follows

$$g(z)=f'(z) \quad (8)$$

The integrals defined in the above equations shall be resolved by a type method and can be written as follows

$$\begin{gathered}\int\theta(x,y,t)\,dx=A'\frac{\partial\theta(x,y,t)}{\partial x};\int\theta(x,y,t)\,dy=B'\frac{\partial\theta(x,y,t)}{\partial y};\\ k_1A'\frac{\partial\theta(x,y,t)}{\partial x}=\varphi_x(x,y,t);k_2B'\frac{\partial\theta(x,y,t)}{\partial y}=\varphi_y(x,y,t)\end{gathered} \quad (9)$$

where the coefficients A' and B' are expressed according to the type of solution used, in this case for exact solutions for sandwich plates for different boundary conditions. Therefore, A', B', k_1 and k_2 are expressed as follows.

where λ and μ are defined in section 3.

For elastic and isotropic FGMs, the constitutive relations can be written as

$$\begin{Bmatrix}\sigma_x\\ \sigma_y\\ \tau_{xy}\end{Bmatrix}^{(n)}=\begin{bmatrix}Q_{11}&Q_{12}&0\\ Q_{12}&Q_{22}&0\\ 0&0&Q_{66}\end{bmatrix}^{(n)}\begin{Bmatrix}\varepsilon_x\\ \varepsilon_y\\ \gamma_{xy}\end{Bmatrix}^{(n)}\quad\text{and}$$
$$\begin{Bmatrix}\tau_{yz}\\ \tau_{zx}\end{Bmatrix}^{(n)}=\begin{bmatrix}Q_{44}&0\\ 0&Q_{55}\end{bmatrix}^{(n)}\begin{Bmatrix}\gamma_{yz}\\ \gamma_{zx}\end{Bmatrix}^{(n)} \quad (10)$$

Table 1 value of A', B', k_1 and k_2 for different boundary conditions

Boundary conditions	A'	k_1	B'	k_2
SSSS	$-1/\lambda^2$	λ^2	$-1/\mu^2$	μ^2
CSSS	$-1/3\lambda^2$	$3\lambda^2$	$-1/\mu^2$	μ^2
CSCS	$-1/3\lambda^2$	$3\lambda^2$	$-1/3\mu^2$	$3\mu^2$
CCSS	$-1/4\lambda^2$	$4\lambda^2$	$-1/\mu^2$	μ^2
CCCC	$-1/4\lambda^2$	$4\lambda^2$	$-1/4\mu^2$	$4\mu^2$
FFCC	$-1/8\lambda^2$	$8\lambda^2$	$-1/4\mu^2$	$4\mu^2$

where (σ_x, σ_y σ_y, τ_{xy}, τ_{yz}, τ_{yx}) and (ε_x, ε_y, γ_{xy}, γ_{yz}, γ_{yx}) are the stress and strain components, respectively.

Using the material properties defined in Eq. (1), stiffness coefficients, Q_{ij}, can be expressed as

$$Q_{11}^{(n)}=Q_{22}^{(n)}=\frac{E^{(n)}(z)}{1-\nu^2}, \quad (11a)$$

$$Q_{12}^{(n)}=\frac{\nu\,E^{(n)}(z)}{1-\nu^2}, \quad (11b)$$

$$Q_{44}^{(n)}=Q_{55}^{(n)}=Q_{66}^{(n)}=\frac{E^{(n)}(z)}{2(1+\nu)}, \quad (11c)$$

The stress and moment resultants of the FGM sandwich plate can be obtained by integrating Eq. (10)over the thickness, and are written as

$$\begin{Bmatrix}N_x,&N_y,&N_{xy}\\ M_x,&M_y,&M_{xy}\\ S_x,&S_y,&S_{xy}\end{Bmatrix}=\sum_{n=1}^{3}\int_{h_{n-1}}^{h_n}(\sigma_x,\sigma_y,\tau_{xy})^{(n)}\begin{Bmatrix}1\\ z\\ f(z)\end{Bmatrix}dz, \quad (12a)$$

$$(Q_{xz},Q_{yz})=\sum_{n=1}^{3}\int_{h_{n-1}}^{h_n}(\tau_{xz},\tau_{yz})^{(n)}g(z)dz. \quad (12b)$$

where h_n and h_{n-1} are the top and bottom z-coordinates of the nth layer.

Using Eq. (10) in Eqs. (12), the stress resultants of a sandwich plate made up of three layers can be related to the total strains by

$$\begin{Bmatrix}N\\ M\\ S\end{Bmatrix}=\begin{bmatrix}A&B&B^s\\ B&D&D^s\\ B^s&D^s&H^s\end{bmatrix}\begin{Bmatrix}\varepsilon\\ k^b\\ k^s\end{Bmatrix},\quad Q=A^s\gamma \quad (13)$$

where

$$N=\{N_x,N_y,N_{xy}\}^t,\quad M^b=\{M_x,M_y,M_{xy}\}^t,$$
$$M^s=\{S_x,S_y,S_{xy}\}^t \quad (14a)$$

$$\varepsilon=\{\varepsilon_x^0,\varepsilon_y^0,\gamma_{xy}^0\}^t,\quad k^b=\{k_x^b,k_y^b,k_{xy}^b\}^t, \quad (14b)$$
$$k^s=\{k_x^s,k_y^s,k_{xy}^s\}^t$$

$$A=\begin{bmatrix}A_{11}&A_{12}&0\\ A_{12}&A_{22}&0\\ 0&0&A_{66}\end{bmatrix},\ B=\begin{bmatrix}B_{11}&B_{12}&0\\ B_{12}&B_{22}&0\\ 0&0&B_{66}\end{bmatrix},$$
$$D=\begin{bmatrix}D_{11}&D_{12}&0\\ D_{12}&D_{22}&0\\ 0&0&D_{66}\end{bmatrix}, \quad (14c)$$

$$B^s=\begin{bmatrix}B_{11}^s&B_{12}^s&0\\ B_{12}^s&B_{22}^s&0\\ 0&0&B_{66}^s\end{bmatrix},\ D^s=\begin{bmatrix}D_{11}^s&D_{12}^s&0\\ D_{12}^s&D_{22}^s&0\\ 0&0&D_{66}^s\end{bmatrix},$$
$$H^s=\begin{bmatrix}H_{11}^s&H_{12}^s&0\\ H_{12}^s&H_{22}^s&0\\ 0&0&H_{66}^s\end{bmatrix}, \quad (14d)$$

$$S=\{Q_{yz},Q_{xz}\}^t,\quad \gamma=\{\gamma_{yz},\gamma_{xz}\}^t,\quad A^s=\begin{bmatrix}A_{44}^s & 0\\ 0 & A_{55}^s\end{bmatrix},\tag{14e}$$

where A_{ij}, B_{ij}, etc., are the plate stiffness, defined by

$$\begin{Bmatrix}A_{11} & B_{11} & D_{11} & B_{11}^s & D_{11}^s & H_{11}^s\\ A_{12} & B_{12} & D_{12} & B_{12}^s & D_{12}^s & H_{12}^s\\ A_{66} & B_{66} & D_{66} & B_{66}^s & D_{66}^s & H_{66}^s\end{Bmatrix}=$$

$$\sum_{n=1}^{3}\int_{h_{n-1}}^{h_n} Q_{11}^{(n)}\left(1,z,z^2,f(z),z\,f(z),f^2(z)\right)\begin{Bmatrix}1\\ \nu^{(n)}\\ \dfrac{1-\nu^{(n)}}{2}\end{Bmatrix}dz\tag{15a}$$

and

$$\left(A_{22},B_{22},D_{22},B_{22}^s,D_{22}^s,H_{22}^s\right)=\left(A_{11},B_{11},D_{11},B_{11}^s,D_{11}^s,H_{11}^s\right),$$

$$Q_{11}^{(n)}=\frac{E(z)}{1-\nu^2}\tag{15b}$$

$$A_{44}^s=A_{55}^s=\sum_{n=1}^{3}\int_{h_{n-1}}^{h_n}\frac{E(z)}{2(1+\nu)}\left[g(z)\right]^2dz,\tag{15c}$$

2.3 Governing equations

The principle of virtual work is employed for buckling problem of FG sandwich plate. The principle can be expressed in analytical from as

$$\delta U+\delta U_F+\delta V=0\tag{16}$$

Where δU is the virtual strain energy, δU_F additional s train energy induced by the elastic foundations and δV is th e virtual work done by applied forces.

The virtual strain energy is expressed by

$$\begin{aligned}\delta U&=\int_A\int_{-h/2}^{h/2}\left(\sigma_x^{(n)}\delta\varepsilon_x+\sigma_y^{(n)}\delta\varepsilon_y+\tau_{xy}^{(n)}\delta\gamma_{xy}+\tau_{xz}^{(n)}\delta\gamma_{xz}+\tau_{yz}^{(n)}\delta\gamma_{yz}\right)dAdz\\&=\int_A\left[N_x\delta\varepsilon_x^0+N_{xy}\delta\gamma_{xy}^0+N_y\delta\varepsilon_y^0+M_x\delta k_x^b+M_y\delta k_y^b\right.\\&\left.+M_{xy}\delta k_{xy}^b+S_x\delta k_x^s+S_y\delta k_y^s+S_{xy}\delta k_{xy}^s+Q_{yz}\delta\gamma_{yz}^0+Q_{xz}\delta\gamma_{xz}^0\right]dA\end{aligned}\tag{17}$$

where A is the top surface.

The strain energy induced by elastic foundations can be defined as

$$\delta U_F=\int_A f_e\delta w_0dA\tag{18}$$

where A is the area of top surface and f_e is the density of reaction force of foundation. For the visco-Winkler-Pasternak foundations model

$$f_e=k_ww-k_{sx}\frac{\partial^2w}{\partial x^2}-k_{sy}\frac{\partial^2w}{\partial y^2}+c_t\frac{\partial w}{\partial t}\tag{19}$$

where k_w is the modulus of subgrade reaction (elastic coefficient of the foundation) and k_{sx} and k_{sy} are= the shear moduli of the subgrade (shear layer foundation stiffness) and the damping coefficient c_t of the viscoelastic medium.

If foundation is homogeneous and isotropic, we will get $k_{sx}=k_{sy}=k_s$.

The external virtual work due to in-plane forces and shear forces applied to the plate is given as

$$\delta V=-\int_A\left(\overline{N}_{xx}\frac{\partial^2w_0}{\partial x^2}+2\overline{N}_{xy}\frac{\partial^2w_0}{\partial x\partial y}+\overline{N}_{yy}\frac{\partial^2w_0}{\partial y^2}\right)\delta w_0dA\tag{20}$$

being $\overline{N}_{xx}$ and $\overline{N}_{yy}$ the in-plane loads perpendicular to the edges $x=0$ and $y=0$, respectively, and $\overline{N}_{xy}$ and $\overline{N}_{yx}$ the distributed shear forces parallel to the edges $x=0$ and $y=0$, respectively.

Substituting Eqs. (18), (19) and (20) into Eq. (16) and integrating by parts, and collecting the coefficients of $(\delta u_0,\delta v_0,\delta w_0,\delta\theta)$, the following equations of motion are obtained

$$\begin{aligned}&\delta u_0:\frac{\partial N_x}{\partial x}+\frac{\partial N_{xy}}{\partial y}=0\\&\delta v_0:\frac{\partial N_y}{\partial y}+\frac{\partial N_{xy}}{\partial x}=0\\&\delta w_0:\frac{\partial^2M_x}{\partial x^2}+2\frac{\partial^2M_{xy}}{\partial x\partial y}+\frac{\partial^2M_y}{\partial y^2}-\overline{N}-f_e=0\\&\delta\theta:-k_1S_x-k_2S_y-\left(k_1A'+k_2B'\right)\frac{\partial^2S_{xy}}{\partial x\partial y}+k_1A'\frac{\partial Q_{xz}}{\partial x}+k_2B'\frac{\partial Q_{yz}}{\partial y}=0\end{aligned}\tag{21}$$

2.4 Equations of motion in terms of displacements

Substituting Eqs. (7), (13) into Eq. (20), the equations of motion can be expressed in terms of generalized displacements $(\delta u_0,\delta v_0,\delta w_0,\delta\theta)$ as

$$\begin{aligned}&\delta u_0:A_{11}\frac{\partial^2u_0}{\partial x^2}+A_{12}\frac{\partial^2v_0}{\partial x\partial y}+A_{66}\left(\frac{\partial^2u_0}{\partial y^2}+\frac{\partial^2v_0}{\partial x\partial y}\right)-B_{11}\frac{\partial^3w_0}{\partial x^3}\\&-B_{12}\frac{\partial^3w_0}{\partial x\partial y^2}-2B_{66}\frac{\partial^3w_0}{\partial x\partial y^2}+B_{11}^sk_1A'\frac{\partial^3\theta}{\partial x^3}+B_{12}^sk_2B'\frac{\partial^2\theta}{\partial x\partial y^2}\\&+B_{66}^s\left(k_1A'+k_2B'\right)\frac{\partial^3\theta}{\partial x\partial y^2}=0\\&\delta v_0:A_{12}\frac{\partial^2u_0}{\partial x\partial y}+A_{22}\frac{\partial^2v_0}{\partial y^2}+A_{66}\left(\frac{\partial^2u_0}{\partial x\partial y}+\frac{\partial^2v_0}{\partial x^2}\right)-B_{12}\frac{\partial^3w_0}{\partial x^2\partial y}\\&-B_{22}\frac{\partial^3w_0}{\partial y^3}-2B_{66}\frac{\partial^3w_0}{\partial x^2\partial y}+B_{12}^sk_1A'\frac{\partial^3\theta}{\partial x^2\partial y}+B_{22}^sk_2B'\frac{\partial^2\theta}{\partial y^3}\\&+B_{66}^s\left(k_1A'+k_2B'\right)\frac{\partial^3\theta}{\partial x^2\partial y}=0\\&\delta w_0:B_{11}\frac{\partial^3u_0}{\partial x^3}+B_{12}\left(\frac{\partial^3u_0}{\partial x\partial y^2}+\frac{\partial^3v_0}{\partial x^2\partial y}\right)+B_{22}\frac{\partial^3v_0}{\partial y^3}\\&+2B_{66}\left(\frac{\partial^3u_0}{\partial x\partial y^2}+\frac{\partial^3v_0}{\partial x^2\partial y}\right)-D_{11}\frac{\partial^4w_0}{\partial x^4}-2D_{12}\frac{\partial^4w_0}{\partial x^2\partial y^2}\\&-D_{22}\frac{\partial^4w_0}{\partial y^4}-4D_{66}\frac{\partial^4w_0}{\partial x^2\partial y^2}+D_{11}^sk_1A'\frac{\partial^4\theta}{\partial x^4}\\&+D_{12}^s\left(k_1A'+k_2B'\right)\frac{\partial^4\theta}{\partial x^2\partial y^2}+D_{22}^sk_2B'\frac{\partial^4\theta}{\partial y^4}\\&+2D_{66}^s\left(k_1A'+k_2B'\right)\frac{\partial^4\theta}{\partial x^2\partial y^2}+\overline{N}_{xx}\frac{\partial^2w_0}{\partial x^2}+2\overline{N}_{xy}\frac{\partial^2w_0}{\partial x\partial y}+\overline{N}_{yy}\frac{\partial^2w_0}{\partial y^2}\\&+k_ww_0-k_s\left(\frac{\partial^2w_0}{\partial x^2}+\frac{\partial^2w_0}{\partial y^2}\right)+c_t\frac{\partial w_0}{\partial t}=0\end{aligned}\tag{22}$$

$$\delta\theta: -B_{11}^s k_1A' \frac{\partial^3 u_0}{\partial x^3} - B_{12}^s \left(k_1A' \frac{\partial^3 v_0}{\partial x^2 \partial y} + k_2B' \frac{\partial^3 u_0}{\partial x \partial y^2} \right) - B_{22}^s k_2B' \frac{\partial^3 v_0}{\partial y^3}$$
$$+ D_{11}^s k_1A' \frac{\partial^4 w_0}{\partial x^4} - D_{66} \left(k_1A' + k_2B' \right) \left(\frac{\partial^3 u_0}{\partial x \partial y^2} + \frac{\partial^3 v_0}{\partial x^2 \partial y} \right)$$
$$+ \left(k_1A' + k_2B' \right) \left(D_{12}^s + 2D_{66}^s \right) \frac{\partial^4 w_0}{\partial x^2 \partial y^2} + D_{22}^s k_2B' \frac{\partial^4 w_0}{\partial y^4} - H_{11}^s \left(k_1A' \right)^2 \frac{\partial^4 \theta}{\partial x^4}$$
$$- 2H_{12}^s k_1A' k_2B' \frac{\partial^4 \theta}{\partial x^2 \partial y^2} - H_{22}^s \left(k_2B' \right)^2 \frac{\partial^4 \theta}{\partial y^4} - H_{66}^s \left(k_1A' + k_2B' \right) \frac{\partial^4 \theta}{\partial x^2 \partial y^2}$$
$$+ A_{55}^s \left(k_1A' \right)^2 \frac{\partial^2 \theta}{\partial x^2} + A_{44}^s \left(k_2B' \right)^2 \frac{\partial^2 \theta}{\partial y^2} = 0$$

3. Exact solutions for FGMs sandwich plates

In this section, exact solutions of the governing equations for buckling analysis of a EGMs sandwich plate with simply supported (S), clamped (C) or free (F) edges are presented. These boundary conditions are defined as follow:

Simply supported (S)

$$\begin{aligned} v_0 = w_0 = \frac{\partial \theta}{\partial y} = N_{xx} = M_{xx} = S_{xx} = 0 \qquad at \qquad x = 0, a, \\ u_0 = w_0 = \frac{\partial \theta}{\partial x} = N_{yy} = M_{yy} = S_{yy} = 0 \qquad at \qquad y = 0, b. \end{aligned} \tag{23}$$

Clamped (C)

$$u_0 = v_0 = w_0 = \frac{\partial \theta}{\partial x} = \frac{\partial \theta}{\partial y} = 0 \quad at \qquad x = 0, a; \qquad y = 0, b. \tag{24}$$

Free (F)

$$\begin{aligned} M_{xx} = M_{xy} = Q_{xz} = 0 \qquad at \qquad x = 0, a, \\ M_{yy} = M_{xy} = Q_{yz} = 0 \qquad at \qquad y = 0, b. \end{aligned} \tag{25}$$

The following representation for the displacement quant ities, that satisfy the above boundary conditions, is appropri ate in the case of our problem

$$\begin{Bmatrix} u_0 \\ v_0 \\ w_0 \\ \theta \end{Bmatrix} = \sum_{m=1}^{\infty} \sum_{n=1}^{\infty} \begin{Bmatrix} U_{mn} e^{i\omega t} \dfrac{\partial X_m(x)}{\partial x} Y_n(y) \\ V_{mn} e^{i\omega t} X_m(x) \dfrac{\partial Y_n(y)}{\partial y} \\ W_{mn} e^{i\omega t} X_m(x) Y_n(y) \\ Z_{mn} e^{i\omega t} \dfrac{\partial^2 X_m(x)}{\partial x^2} Y_n(y) \end{Bmatrix} \tag{26}$$

Where U_{mn}, V_{mn}, W_{mn} and Z_{mn}, are arbitrary coefficients to be determined. The functions $X_m(x)$ and $Y_n(y)$ are suggested here to satisfy at least the geometric boundary conditions given in Eqs.(23)-(25) and represent approximate shapes of the deflected surface of the plate. These functions, for the different cases of boundary conditions, are listed in Table 2 noting that $\lambda = m\pi/a$, $\mu = n\pi/b$. The plate is subjected to an in-plane forces sin two directions $\bar{N}_x = N_{cr}$, $\bar{N}_y = \chi N_{cr}$ i.e., $\chi = \bar{N}_y / \bar{N}_x$ and $\bar{N}_{xy} = 0$.

Substituting expressions (26) into the governing Eqs. (22) and multiplying each equation by the corresponding eigenfunction then integrating over the domain of solution, we can obtain, after some mathematical manipulations, the following equations

$$\begin{bmatrix} S_{11} & S_{12} & S_{13} & S_{14} \\ S_{21} & S_{22} & S_{23} & S_{24} \\ S_{31} & S_{32} & S_{33} & S_{34} \\ S_{41} & S_{42} & S_{43} & S_{44} \end{bmatrix} \begin{Bmatrix} U_{mn} \\ V_{mn} \\ W_{mn} \\ Z_{mn} \end{Bmatrix} = 0 \tag{27}$$

in which

$$\begin{aligned} S_{11} &= A_{11} e_{12} + A_{66} e_8 \\ S_{12} &= \left(A_{12} + A_{66} \right) e_8 \\ S_{13} &= -\left(B_{12} + 2B_{66} \right) e_8 - B_{11} e_{12} \\ S_{14} &= \left[k_1A' B_{66}^s + k_2B' \left(B_{12}^s + B_{66}^s \right) \right] e_8 + k_1A' B_{11}^s e_{12} \\ S_{21} &= \left(A_{12} + A_{66} \right) e_{10} \\ S_{22} &= A_{22} e_4 + A_{66} e_{10} \\ S_{23} &= \left(B_{12} + 2B_{66} \right) e_{10} - B_{22} e_4 \\ S_{24} &= \left[k_1A' \left(B_{12}^s + B_{66}^s \right) + k_2B' B_{66}^s \right] e_{10} + k_2B' B_{22}^s e_4 \end{aligned}$$

$$\begin{aligned} S_{31} &= \left(B_{12} + 2B_{66} \right) e_{11} - B_{11} e_{13} \\ S_{32} &= \left(B_{12} + 2B_{66} \right) e_{11} - B_{22} e_5 \\ S_{33} &= \left(-2D_{12} + 4D_{66} \right) e_{11} - D_{11} e_{13} - D_{22} e_5 + \left(\bar{N}_{xx} - k_{sx} \right) e_9 \\ &\quad + \left(\bar{N}_{yy} - k_{sy} \right) e_3 + \left(k_w + c_t \omega \right) e_1 + 2\bar{N}_{xy} e_7 \\ S_{34} &= \left[k_1A' \left(D_{11}^s + 2D_{66}^s \right) + k_2B' \left(D_{12}^s + 2D_{66}^s \right) \right] e_{11} \\ &\quad + k_1A' D_{11}^s e_{13} + k_2B' D_{22}^s e_5 \\ S_{41} &= -\left[k_1A' B_{66}^s + k_2B' \left(B_{12}^s - B_{66}^s \right) \right] e_{11} - k_1A' B_{11}^s e_{13} \\ S_{42} &= -\left[k_1A' \left(B_{12}^s + 2B_{66}^s \right) e_{11} + k_2B' \left(B_{66}^s e_{11} + B_{22}^s e_5 \right) \right] \\ S_{43} &= [k_1A' (D_{11}^s + 2D_{66}^s) + k_2B' (D_{12}^s + 2D_{66}^s)] e_{11} + k_1A' D_{11}^s e_{13} \\ &\quad + k_2B' D_{22}^s e_5 \\ S_{44} &= \left(H_{11}^s \left(k_1A' \right)^2 + 2H_{12}^s k_1A' k_2B' + H_{11}^s \left(k_2B' \right)^2 \right) e_{15} \\ &\quad + H_{66}^s \left(k_1A' + k_2B' \right)^2 e_{18} - A_{55}^s \left(\left(k_1A' \right)^2 e_{19} + \left(k_2B' \right)^2 e_{16} \right) \end{aligned} \tag{28}$$

With

$$\begin{aligned} (e_{20}, e_8, e_{12}) &= \int_0^b \int_0^a \left(X_m''' Y_n'', X_m' Y_n'', X_m''' Y_n \right) X_m' Y_n \, dx dy \\ (e_{21}, e_4, e_{10}) &= \int_0^b \int_0^a \left(X_m''' Y_n', X_m Y_n''', X_m'' Y_n' \right) X_m Y_n' \, dx dy \\ (e_1, e_3, e_5, e_{14}) &= \int_0^b \int_0^a \left(X_m Y_n, X_m Y_n'', X_m Y_n'''', X_m'''' Y_n'' \right) X_m Y_n \, dx dy \\ (e_7, e_9, e_{11}, e_{13}) &= \int_0^b \int_0^a \left(X_m' Y_n', X_m'' Y_n, X_m'' Y_n'', X_m'''' Y_n \right) X_m Y_n \, dx dy \\ (e_{15}, e_{16}, e_{17}) &= \int_0^b \int_0^a \left(X_m'' Y_n, X_m'' Y_n'', X_m Y_n'' \right) X_m'' Y_n \, dx dy \\ (e_{18}, e_{19}) &= \int_0^b \int_0^a \left(X_m'''' Y_n'', X_m'''' Y_n \right) X_m'' Y_n \, dx dy \end{aligned} \tag{29}$$

As can be clearly seen from Eq. (29), the coefficient S_{33} is a function of the normal loads applied to the edges of the plate, i.e., $\bar{N}_{xx}$ and $\bar{N}_{yy}$. The matrix system (28) has a non-trivial solution if, and only if, its determinant $|S_{ij}|$ is equal to zero. The critical buckling load is thus obtained.

4. Numerical results and discussions

In this section, the accuracy of the presented plate theory for the buckling analysis of symmetric rectangular

Table 2 The admissible functions $X_m(x)$ and $Y_n(y)$

Boundary conditions			The functions $X_m(x)$ and $Y_n(y)$	
SSSS	$X_m(0)=X''_m(0)=0$ $X_m(a)=X''_m(a)=0$	$Y_n(0)=Y''_n(0)=0$ $Y_n(b)=Y''_n(b)=0$	$\sin(\lambda x)$	$\sin(\mu y)$
CSSS	$X_m(0)=X'_m(0)=0$ $X_m(a)=X''_m(a)=0$	$Y_n(0)=Y''_n(0)=0$ $Y_n(b)=Y''_n(b)=0$	$\sin(\lambda x)[\cos(\lambda x)-1]$	$\sin(\mu y)$
CSCS	$X_m(0)=X'_m(0)=0$ $X_m(a)=X''_m(a)=0$	$Y_n(0)=Y'_n(0)=0$ $Y_n(b)=Y''_n(b)=0$	$\sin(\lambda x)[\cos(\lambda x)-1]$	$\sin(\mu y)[\cos(\mu y)-1]$
CCSS	$X_m(0)=X'_m(0)=0$ $X_m(a)=X'_m(a)=0$	$Y_n(0)=Y''_n(0)=0$ $Y_n(b)=Y''_n(b)=0$	$\sin^2(\lambda x)$	$\sin(\mu y)$
CCCC	$X_m(0)=X'_m(0)=0$ $X_m(a)=X'_m(a)=0$	$Y_n(0)=Y'_n(0)=0$ $Y_n(b)=Y'_n(b)=0$	$\sin^2(\lambda x)$	$\sin^2(\mu y)$
FFCC	$X''_m(0)=X'''_m(0)=0$ $X''_m(a)=X'''_m(a)=0$	$Y_n(0)=Y'_n(0)=0$ $Y_n(b)=Y'_n(b)=0$	$\cos^2(\lambda x)[\sin^2(\lambda x)+1]$	$sin^2(\mu y)$

– ( )' denotes the derivative with respect to the corresponding coordinates

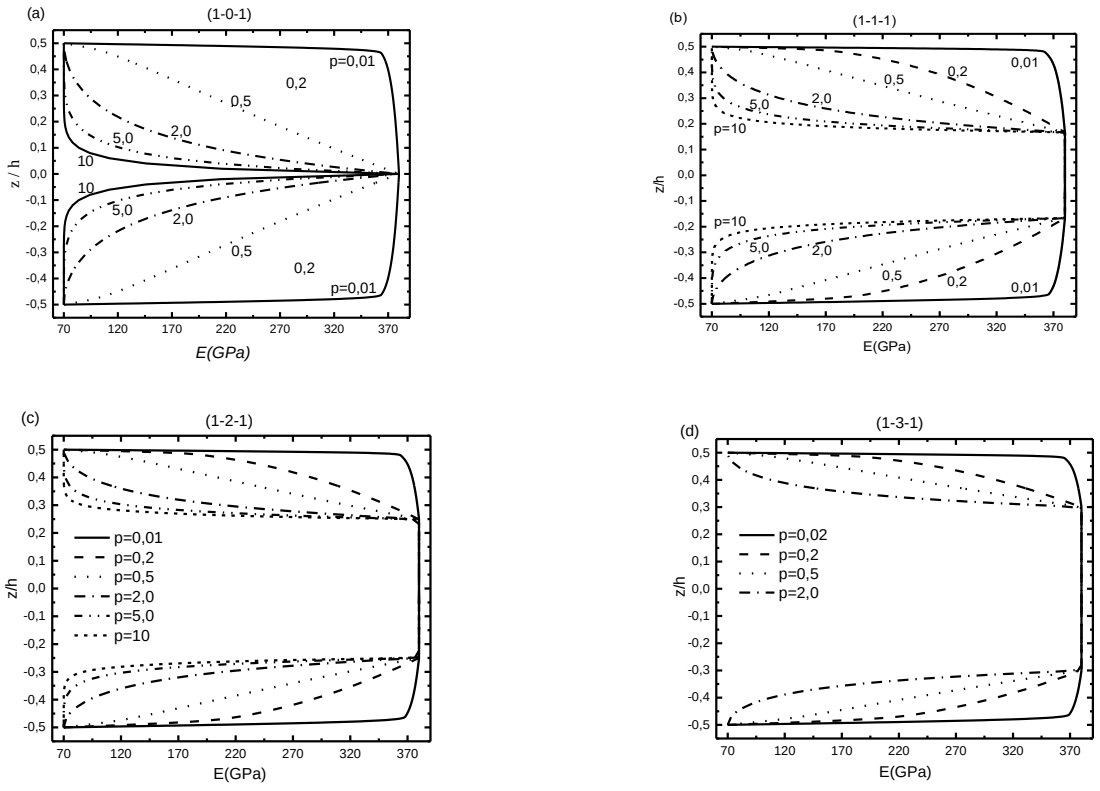

Fig. 3 Variation of the Young's modulus through plate thickness of symmetric sandwich plates for various values of the po wer-law index p: (a) The (1-0-1) EGM sandwich plate, (b) The (1-1-1) EGM sandwich plate, (c) The (1-2-1) EGM sandwic h plate and (d) The (1-3-1) EGM sandwich plate

EGM sandwich plates resting on two-parameter elastic foundations with various cases of the boundary conditions is demonstrated by comparing the analytical solution with those of other available results in the literature.

The combination of materials consists of aluminum and alumina with the following material properties:

- Ceramic (alumina, Al_2O_3): $E_c = 380\ GPa, \nu_c = 0.3$
- Metal (aluminum, Al): $E_m = 70\ GPa, \nu_m = 0.3$

In the following, we note that several kinds of sandwich plates are used:

- The (1-0-1) FG sandwich plate: The plate is symmetric and made of only two equal-thickness FG layers, i.e., there is no core layer. Thus, we have, $h_1 = h_2 = 0$

Table 3 Comparison of critical buckling load $\bar{N}$ of simply supported EGM sandwich square plates (k=1.5) resting on Visco-Pasternak's elastic foundations

Scheme	Theory	$\bar{c}_t$	$\bar{K}_w = \bar{K}_s = 0$			$\bar{K}_w = 100, \bar{K}_s = 0$			$\bar{K}_w = \bar{K}_s = 100$		
			a/h = 5	10	20	a/h = 5	10	20	a/h = 5	10	20
1–0–1	FPT[a]	$\bar{c}_t = 0$	2.5154	2.7987	2.8797	4.2783	4.5616	4.6427	39.0768	39.3601	39.4412
	TPT[a]	$\bar{c}_t = 0$	2.5592	2.8119	2.8832	4.3220	4.5748	4.6461	39.1206	39.3734	39.4447
	SPT[a]	$\bar{c}_t = 0$	2.5618	2.8127	2.8834	4.3247	4.5756	4.6463	39.1232	39.3741	39.4449
	EPT[a]	$\bar{c}_t = 0$	2.5652	2.8137	2.8837	4.3281	4.5766	4.6466	39.1266	39.3752	39.4451
	HPT[a]	$\bar{c}_t = 0$	2.5834	2.8193	2.8852	4.3463	4.5822	4.6481	39.1448	39.3808	39.4466
	Model 1[b]	$\bar{c}_t = 0$	2.5618	2.8127	2.8834	4.3247	4.5756	4.6463	39.1232	39.3741	39.4449
	Model 2[b]	$\bar{c}_t = 0$	2.5592	2.8120	2.8833	4.3221	4.5749	4.6462	39.1206	39.3734	39.4447
	Present	$\bar{c}_t = 0$	2.5647	2.8136	2.8837	4.3276	4.5765	4.6466	39.1262	39.3750	39.4452
		$\bar{c}_t = 0.05$	3.0054	3.2543	3.3244	4.7683	5.0172	5.0873	39.5669	39.8158	39.8859
		$\bar{c}_t = 0.1$	3.4462	3.6950	3.7652	5.2091	5.4580	5.5281	40.0076	40.2565	40.3266
		$\bar{c}_t = 1$	11.3793	11.6282	11.6983	13.1422	13.3911	13.4612	47.9407	48.1896	48.2597
1–1–1	FPT[a]	$\bar{c}_t = 0$	3.0560	3.4014	3.5003	4.8189	5.1643	5.2632	39.6175	39.9628	40.0617
	TPT[a]	$\bar{c}_t = 0$	3.1014	3.4151	3.5039	4.8643	5.1781	5.2668	39.6629	39.9766	40.0653
	SPT[a]	$\bar{c}_t = 0$	3.1030	3.4156	3.5040	4.8659	5.1785	5.2669	39.6644	39.9770	40.0655
	EPT[a]	$\bar{c}_t = 0$	3.1054	3.4163	3.5042	4.8683	5.1792	5.2671	39.6668	39.9777	40.0656
	HPT[a]	$\bar{c}_t = 0$	3.1399	3.4269	3.5070	4.9029	5.1898	5.2699	39.7014	39.9883	40.0684
	Model 1	$\bar{c}_t = 0$	3.1030	3.4156	3.5040	4.8659	5.1785	5.2669	39.6644	39.9770	40.0655
	Model 2	$\bar{c}_t = 0$	3.1015	3.4152	3.5039	4.8644	5.1781	5.2668	39.6629	39.9766	40.0654
	Present	$\bar{c}_t = 0$	3.1051	3.4162	3.5042	4.8680	5.1791	5.2671	39.6665	39.9777	40.0657
		$\bar{c}_t = 0.05$	3.5458	3.8570	3.9449	5.3087	5.6199	5.7078	40.1072	40.4184	40.5064
		$\bar{c}_t = 0.1$	3.9865	4.2977	4.3857	5.7494	6.0606	6.1486	40.5480	40.8591	40.9471
		$\bar{c}_t = 1$	11.9196	12.2308	12.3188	13.6826	13.9937	14.0817	48.4811	48.7922	48.8802
1–2–1	FPT[a]	$\bar{c}_t = 0$	3.4772	3.8906	4.0097	5.2401	5.6535	5.7726	40.0386	40.4520	40.5712
	TPT[a]	$\bar{c}_t = 0$	3.5165	3.9026	4.0129	5.2795	5.6655	5.7758	40.0780	40.4641	40.5744
	SPT[a]	$\bar{c}_t = 0$	3.5165	3.9026	4.0129	5.2795	5.6655	5.7758	40.0780	40.4640	40.5744
	EPT[a]	$\bar{c}_t = 0$	3.5176	3.9028	4.0130	5.2805	5.6657	5.7759	40.0790	40.4643	40.5744
	HPT[a]	$\bar{c}_t = 0$	3.5799	3.9220	4.0180	5.3429	5.6850	5.7810	40.1414	40.4835	40.5795
	Model 1[b]	$\bar{c}_t = 0$	3.5165	3.9026	4.0129	5.2795	5.6655	5.7758	40.0780	40.4640	40.5744
	Model 2[b]	$\bar{c}_t = 0$	3.5166	3.9027	4.0130	5.2795	5.6656	5.7759	40.0780	40.4641	40.5744
	Present	$\bar{c}_t = 0$	3.5174	3.9028	4.0130	5.2804	5.6658	5.7759	40.0789	40.4643	40.5745
		$\bar{c}_t = 0.05$	3.9582	4.3436	4.4537	5.7211	6.1065	6.2167	40.5196	40.9050	41.0152
		$\bar{c}_t = 0.1$	4.3989	4.7843	4.8945	6.1618	6.5472	6.6574	40.9604	41.3457	41.4559
		$\bar{c}_t = 1$	12.3320	12.7174	12.8276	14.0949	14.4803	14.5905	48.8935	49.2789	49.3890
1–3–1	FPT[a]	$\bar{c}_t = 0$	3.7922	4.2636	4.4004	5.5551	6.0265	6.1633	40.3537	40.8251	40.9618
	TPT[a]	$\bar{c}_t = 0$	3.8253	4.2738	4.4031	5.5882	6.0367	6.1660	40.3867	40.8353	40.9645
	SPT[a]	$\bar{c}_t = 0$	3.8243	4.2734	4.4030	5.5872	6.0364	6.1659	40.3857	40.8349	40.9644
	EPT[a]	$\bar{c}_t = 0$	3.8245	4.2734	4.4030	5.5875	6.0364	6.1659	40.3860	40.8349	40.9644
	HPT[a]	$\bar{c}_t = 0$	3.9114	4.3004	4.4101	5.6743	6.0364	6.1730	40.4728	40.8619	40.9716
	Model 1[b]	$\bar{c}_t = 0$	3.8243	4.2734	4.4030	5.5872	6.0364	6.1659	40.3857	40.8349	40.9644
	Model 2[b]	$\bar{c}_t = 0$	3.8253	4.2738	4.4031	5.5882	6.0368	6.1660	40.3868	40.8353	40.9646
	Present	$\bar{c}_t = 0$	3.8245	4.2735	4.4030	5.5874	6.0364	6.1659	40.3860	40.8349	40.9645
		$\bar{c}_t = 0.05$	4.2652	4.7142	4.8437	6.0282	6.4771	6.6067	40.8267	41.2757	41.4052
		$\bar{c}_t = 0.1$	4.7060	5.1550	5.2845	6.4689	6.9179	7.0474	41.2674	41.7164	41.8459
		$\bar{c}_t = 1$	12.6391	13.0881	13.2176	14.4020	14.8510	14.9805	49.2005	49.6495	49.7790

(a) Taken from Sobhy (2013)
(b) Taken from Ait Amar Meziane *et al.* (2014)
(c) EPT: exponential shear deformation plate theory; FPT: first-order shear deformation plate theory; HPT: hyperbolic shear deformation plate theory; SPT: sinusoidal shear deformation plate theory; TPT: third order shear deformation plate theory

- The (1-1-1) FG sandwich plate: Here, the plate is symmetric and made of three equal-thickness layers. In this case, we have, $h_1 = -h/6$, $h_2 = h/6$
- The (1-2-1) FG sandwich plate: The plate is symmetric and we have: $h_1 = -h/4$, $h_2 = h/4$
- The (1-3-1) FG sandwich plate: The plate is symmetric and we have: $h_1 = -3h/10$, $h_2 = 3h/10$

Fig. 3 shows the through-the-thickness variation of the of Young's modulus for p=0.01, 0.2, 0.5, 2, 5 and 10.

For convenience, the following non-dimensional forms are used

$$\bar{N}_{cr} = \frac{N_{cr}a^2}{100h^3}, K_w = \frac{k_w a^4}{D}, K_s = \frac{k_{sx}a^2}{D} = \frac{k_{sy}b^2}{D},$$

$$D = \frac{E_c h^3}{12(1-\nu^2)}$$

Table 3 gives the nondimensionalized values of the buckling load $\bar{N}$ of various types of simply supported sandwich square plates resting on Visco-Pasternak's elastic foundations. The results are compared with those obtained by Sobhy (2013) using various shear deformation plate theories where a well agreement is achieved between the present solutions using a new theory of refined trigonometric shear deformation and the published ones. It can be observed from Table 3 that the increase of the core thickness of the EGM sandwich plates lead to the increase of buckling load, except for the case of the plates resting on Pasternak's foundations where the variation of them is reversed. In addition, the buckling load is increasing with the existence of the elastic foundations. The inclusion of the Pasternak's foundation parameters gives results more than those with the inclusion of Winkler's foundation parameter.

To demonstrate the effect of damping coefficients and to validate the present formulation for plates resting on an

Table 4 Comparison of critical buckling load $\bar{N}$ of (1–1–1) EGM sandwich plates with various boundary conditions ($b/a = 2, \bar{K}_w = \bar{K}_s = 10$)

B.C.	Theory	$\bar{c}_t$	$k = 0$			$k = 0.5$			$k = 3.5$		
			a/h = 5	10	20	a/h = 5	10	20	a/h = 5	10	20
FFCC	FPT[a]	$\bar{c}_t = 0$	15.2693	20.4469	22.5889	10.5119	12.7398	13.5537	7.5375	8.4498	8.7524
	TPT[a]	$\bar{c}_t = 0$	15.3100	20.4524	22.5893	10.7685	12.8483	13.5856	7.5375	8.5326	8.7755
	SPT[a]	$\bar{c}_t = 0$	15.3262	20.4573	22.5906	10.7791	12.8519	13.5866	7.7767	8.5375	8.7769
	EPT[a]	$\bar{c}_t = 0$	15.3581	20.4701	22.5943	10.7947	12.8576	13.5882	7.7922	8.5427	8.7783
	HPT[a]	$\bar{c}_t = 0$	16.4396	21.0333	22.7718	10.9820	12.9404	13.6126	7.7130	8.5156	8.7709
	Model 1[b]	$\bar{c}_t = 0$	15.7316	20.6940	22.6679	10.9709	12.9380	13.6121	7.8557	8.5665	8.7850
	Model 2[b]	$\bar{c}_t = 0$	15.7165	20.6896	22.6667	10.9609	12.9346	13.6112	7.8423	8.5621	8.7838
	Present	$\bar{c}_t = 0$	15.7574	20.7039	22.6707	10.9835	12.9424	13.6133	7.8682	8.5707	8.7861
		$\bar{c}_t = 0.05$	16.3345	21.2810	23.2478	11.5606	13.5195	14.1905	8.4453	9.1478	9.3632
		$\bar{c}_t = 0.1$	16.9116	21.8581	23.8249	12.1377	14.0966	14.7676	9.0224	9.7249	9.9403
		$\bar{c}_t = 1$	27.2996	32.2461	34.2129	22.5257	24.4846	25.1556	19.4104	20.1129	20.3283
CCCC	FPT[a]	$\bar{c}_t = 0$	12.9480	15.8035	16.8213	8.9602	10.1273	10.5061	6.5737	7.0322	7.1710
	TPT[a]	$\bar{c}_t = 0$	12.9640	14.8053	16.8214	9.1032	10.1789	10.5205	6.6922	7.0708	7.1813
	SPT[a]	$\bar{c}_t = 0$	12.9719	15.8075	16.8220	9.1086	10.1806	10.5209	6.6994	7.0730	7.1819
	EPT[a]	$\bar{c}_t = 0$	12.9892	15.8136	16.8237	9.1167	10.1833	10.5216	6.7073	7.0754	7.1826
	HPT[a]	$\bar{c}_t = 0$	13.6482	16.0906	16.9044	9.2238	10.2228	10.5326	6.6669	7.0629	7.1792
	Model 1[b]	$\bar{c}_t = 0$	13.0716	15.8553	16.8365	9.1520	10.1974	10.5257	6.7161	7.0785	7.1835
	Model 2[b]	$\bar{c}_t = 0$	13.0640	15.8532	16.8360	9.1467	10.1958	10.5252	6.7091	7.0764	7.1829
	Present	$\bar{c}_t = 0$	13.0857	15.8602	16.8379	9.1587	10.1996	10.5263	6.7227	7.0805	7.1840
		$\bar{c}_t = 0.05$	13.6146	16.3891	17.3668	9.6876	10.7285	11.0551	7.2515	7.6094	7.7129
		$\bar{c}_t = 0.1$	14.1435	16.9180	17.8956	10.2165	11.2573	11.5840	7.7804	8.1383	8.2417
		$\bar{c}_t = 1$	23.6632	26.4377	27.4154	19.7362	20.7771	21.1038	17.3001	17.6580	17.7615
CSCS	FPT[a]	$\bar{c}_t = 0$	10.8802	12.4597	12.9692	7.6668	8.2896	8.4768	5.8071	6.0450	6.1130
	TPT[a]	$\bar{c}_t = 0$	10.8866	12.4603	12.9692	7.7464	8.3154	8.4837	5.8704	6.0641	6.1180
	SPT[a]	$\bar{c}_t = 0$	10.8906	12.4613	12.9695	7.7493	8.3163	8.4840	5.8742	6.0652	6.1183
	EPT[a]	$\bar{c}_t = 0$	10.9001	12.4644	12.9703	7.7536	8.3176	8.4843	5.8783	6.0663	6.1186
	HPT[a]	$\bar{c}_t = 0$	11.2895	12.6060	13.0096	7.8139	8.3374	8.4896	5.8572	6.0602	6.1170
	Model 1[b]	$\bar{c}_t = 0$	10.9052	12.4673	12.9712	7.7552	8.3183	8.4846	5.8764	6.0659	6.1185
	Model 2[b]	$\bar{c}_t = 0$	10.9012	12.4662	12.9709	7.7523	8.3175	8.4843	5.8726	6.0648	6.1182
	Present	$\bar{c}_t = 0$	10.9131	12.4698	12.9719	7.7588	8.3194	8.4848	5.8799	6.0669	6.1188
		$\bar{c}_t = 0.05$	11.3538	12.9105	13.4126	8.1996	8.7601	8.9256	6.3206	6.5076	6.5595
		$\bar{c}_t = 0.1$	11.7945	13.3512	13.8533	8.6403	9.2009	9.3663	6.7613	6.9483	7.0002
		$\bar{c}_t = 1$	19.7276	21.2843	21.7865	16.5734	17.1340	17.2994	14.6944	14.8814	14.9333
CCSS	FPT[a]	$\bar{c}_t = 0$	12.7243	15.4988	16.4857	8.8365	9.9698	10.3370	6.5105	6.9555	7.0900
	TPT[a]	$\bar{c}_t = 0$	12.7398	15.5004	16.4858	8.9755	10.0199	10.3509	6.6256	6.9929	7.1000
	SPT[a]	$\bar{c}_t = 0$	12.7474	15.5026	16.4864	8.9808	10.0215	10.3514	6.6326	6.9950	7.1006
	EPT[a]	$\bar{c}_t = 0$	12.7642	15.5085	16.4880	8.9886	10.0241	10.3521	6.6402	6.9974	7.1012
	HPT[a]	$\bar{c}_t = 0$	13.4052	15.7773	16.5662	9.0927	10.0624	10.3627	6.6010	6.9853	7.0980
	Model 1[b]	$\bar{c}_t = 0$	12.9080	15.5750	16.5080	9.0485	10.0467	10.3584	6.6581	7.0033	7.1028
	Model 2[b]	$\bar{c}_t = 0$	12.9010	15.5729	16.5074	9.0435	10.0451	10.3580	6.6514	7.0013	7.1023
	Present	$\bar{c}_t = 0$	12.9215	15.5796	16.5092	9.0550	10.0487	10.3590	6.6644	7.0052	7.1033
		$\bar{c}_t = 0.05$	13.4782	16.1363	17.0659	9.6117	10.6054	10.9157	7.2211	7.5619	7.6601
		$\bar{c}_t = 0.1$	14.0350	16.6930	17.6227	10.1684	11.1621	11.4724	7.7778	8.1186	8.2168
		$\bar{c}_t = 1$	24.0557	26.7138	27.6434	20.1892	21.1829	21.4932	17.7986	18.1394	18.2375
CSSS	FPT[a]	$\bar{c}_t = 0$	10.6131	12.0668	12.5311	7.5143	8.0853	8.2557	5.7275	5.9451	6.0069
	TPT[a]	$\bar{c}_t = 0$	10.6189	12.0673	12.5311	7.5876	8.1089	8.2620	5.7856	5.9624	6.0114
	SPT[a]	$\bar{c}_t = 0$	10.6225	12.0683	12.5314	7.5902	8.1096	8.2622	5.7891	5.9634	6.0117
	EPT[a]	$\bar{c}_t = 0$	10.6312	12.0711	12.5321	7.5942	8.1108	8.2625	5.7928	5.9645	6.0120
	HPT[a]	$\bar{c}_t = 0$	10.9920	12.2004	12.5678	7.6497	8.1289	8.2674	5.7735	5.9589	6.0105
	Model 1[b]	$\bar{c}_t = 0$	10.6425	12.0761	12.5336	7.5981	8.1123	8.2630	5.7919	5.9643	6.0120
	Model 2[b]	$\bar{c}_t = 0$	10.6389	12.0752	12.5334	7.5955	8.1116	8.2628	5.7885	5.9633	6.0117
	Present	$\bar{c}_t = 0$	10.6497	12.0784	12.5342	7.6015	8.1133	8.2632	5.7951	5.9652	6.0122
		$\bar{c}_t = 0.05$	11.1262	12.5549	13.0107	8.0779	8.5898	8.7397	6.2716	6.4417	6.4887
		$\bar{c}_t = 0.1$	11.6026	13.0313	13.4871	8.5544	9.0662	9.2162	6.7480	6.9182	6.9651
		$\bar{c}_t = 1$	20.1790	21.6077	22.0635	17.1307	17.6426	17.7925	15.3244	15.4945	15.5415

Table 4 Continued

B.C.	Theory	$\bar{c}_t$	$k = 0$			$k = 0.5$			$k = 3.5$		
			a/h = 5	10	20	a/h = 5	10	20	a/h = 5	10	20
SSSS	FPT[a]	$\bar{c}_t = 0$	7.5245	7.9088	8.0175	5.7741	5.9182	5.9575	4.8112	4.8643	4.8784
	TPT[a]	$\bar{c}_t = 0$	7.5252	7.9089	8.0175	5.7935	5.9237	5.9590	4.8259	4.8683	4.8795
	SPT[a]	$\bar{c}_t = 0$	7.5261	7.9091	8.0175	5.7942	5.9239	5.9590	4.8267	4.8685	4.8795
	EPT[a]	$\bar{c}_t = 0$	7.5284	7.9097	8.0177	5.7952	5.9242	5.9591	4.8277	4.8688	4.8796
	HPT[a]	$\bar{c}_t = 0$	7.6317	7.9407	8.0258	5.8101	5.9284	5.9602	4.8229	4.8675	4.8792
	Model 1[b]	$\bar{c}_t = 0$	7.5261	7.9091	8.0175	5.7942	5.9239	5.9590	4.8267	4.8685	4.8795
	Model 2[b]	$\bar{c}_t = 0$	7.5253	7.9089	8.0175	5.7936	5.9238	5.9590	4.8259	4.8684	4.8795
	Present	$\bar{c}_t = 0$	7.5281	7.9097	8.0177	5.7951	5.9242	5.9591	4.8276	4.8688	4.8796
		$\bar{c}_t = 0.05$	8.2332	8.6148	8.7229	6.5003	6.6294	6.6643	5.5327	5.5740	5.5848
		$\bar{c}_t = 0.1$	8.9384	9.3200	9.4280	7.2054	7.3345	7.3695	6.2379	6.2791	6.2899
		$\bar{c}_t = 1$	21.6314	22.0130	22.1210	19.8984	20.0275	20.0624	18.9309	18.9721	18.9829

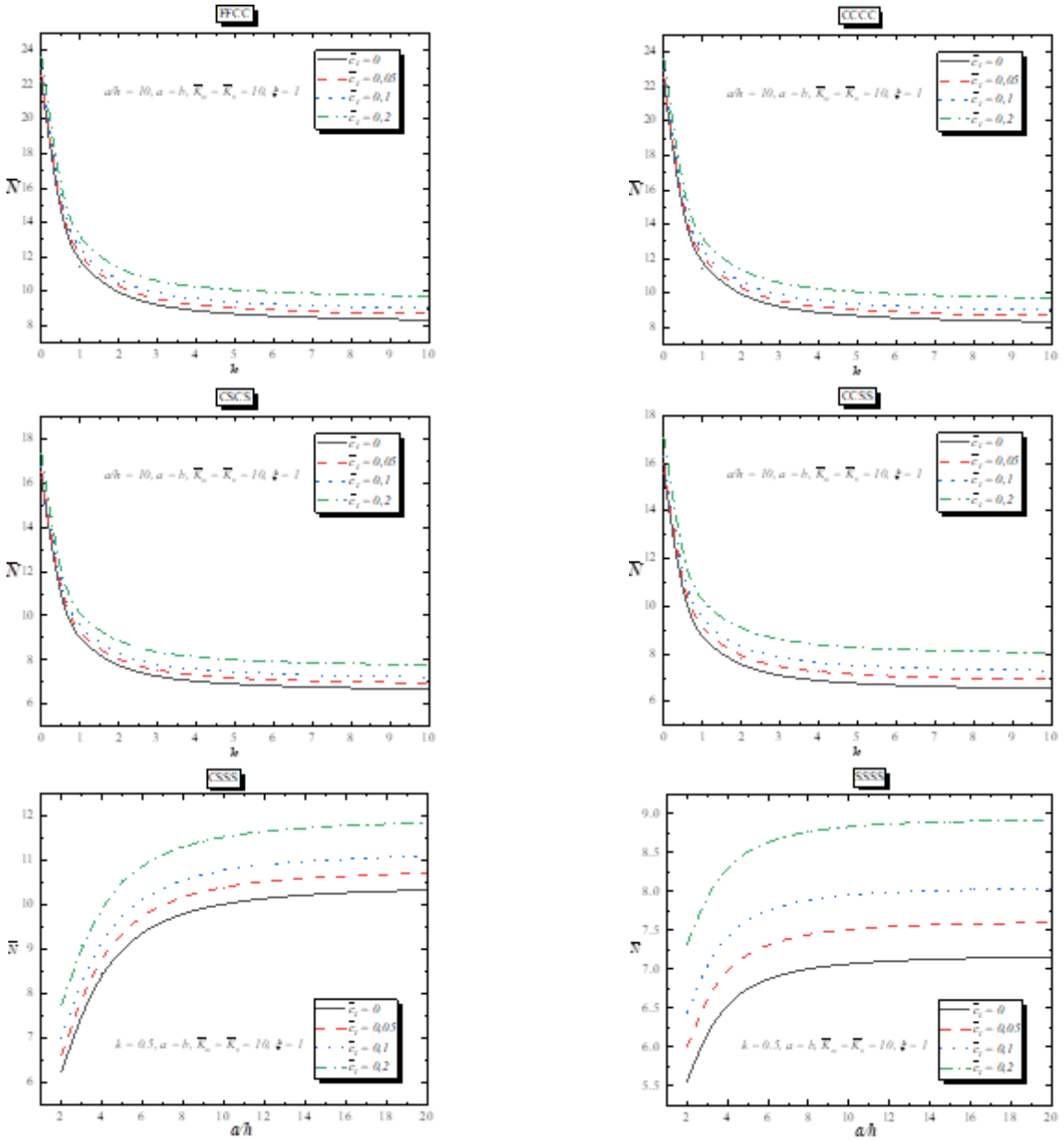

Fig. 4 The variation of non-dimensional Critical buckling $\bar{N}$ versus the gradient index k for different values of damping coefficient of the (1-1-1) FGM sandwich square plates with various boundary conditions

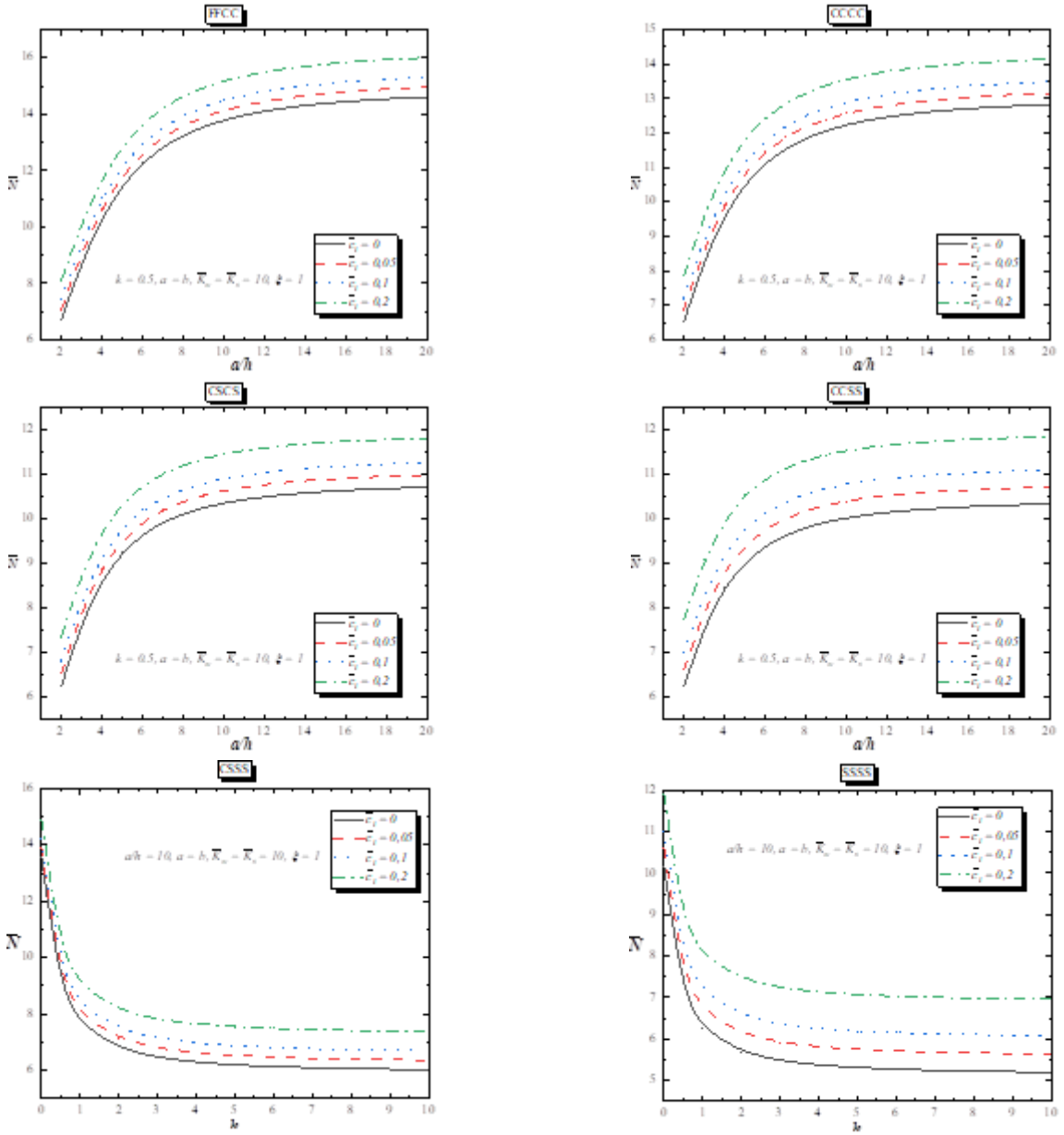

Fig. 5 Critical buckling $\overline{N}$versus the ratio a/h of the (1-1-1) FGM sandwich square plates resting on Visco-Pasternak's elastic foundation with various boundary conditions for different values of damping coefficient.

elastic foundation, the results for dimensionless critical buckling load $\overline{N}$ are presented for square plate simply supported on a visco-Pasternak foundation. The results are compared with those of Sobhy (2013) and of Ait Amar Meziane *et al*. (2014) in the case where the viscosity effect is neglected ($\overline{c}_t = 0$). It is observed that the results agree closely.

However, it is seen that the critical buckling load $\overline{N}$ of the plate is very sensitive to the inclusion of the viscosity effect. The critical buckling load $\overline{N}$ are increasing with the increase of the parameters $\overline{K}_w$, $\overline{K}_s$ and $\overline{c}_t$.

Table 4 contain dimensionless critical buckling load of the (1–1–1) EGM sandwich plate resting on two-parameter elastic foundations under various boundary conditions. The obtained results are compared with those reported by Sobhy (2013) and Ait Amar Meziane *et al.* (2014) using both model 1 and model 2 for different values of the side-to-thickness ratio a/h and inhomogeneity parameter *k*. It can be seen that the results obtained in this study using an efficient and simple theory of refined shear deformation are in good agreement. A decrement for the critical buckling load can be clearly observed with the increase of the parameter *k*. The results are maximum for the free-clamped plates and minimum for the simply supported plates.

In addition to that the critical buckling load of a (1–1–1) EGM sandwich plates with various boundary conditions resting on a visco-Winkler foundation is presented in Table 4. The results obtained in the case where the damping coefficient $\overline{c}_t$ is zero, are compared with those given by Sobhy (2013) and Ait Amar Meziane *et al.* (2014). It is

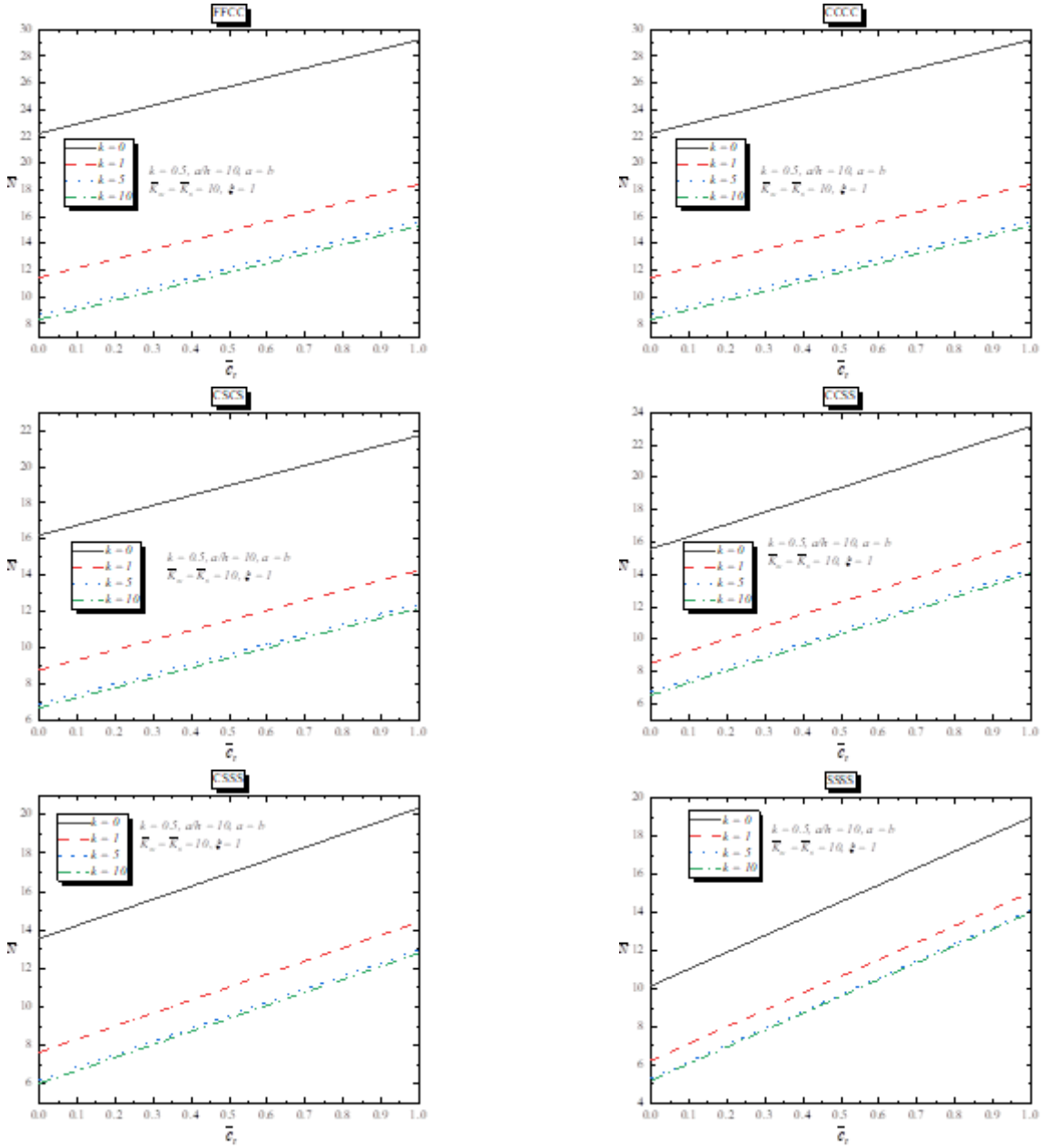

Fig. 6 Effect of damping coefficient for various values of the inhomogeneity parameter k on the non-dimensional critical buckling $\bar{N}$ of the (1-1-1) FGM sandwich square plates with various boundary conditions.

observed that when the viscosity term is omitted, a good agreement between the results is remarked. However, the introduction of the viscosity term increases the critical buckling load because of the damping effect.

Fig. 4 present the variation of the non-dimensional critical buckling$\bar{N}$versus the gradient index k for different values of damping coefficient of the (1-1-1) FGM sandwich square plates with various boundary conditions. The thickness ratio of the plate is considered equal to 10.

It can be observed that increasing the inhomogeneity parameter k leads to a reduction of critical buckling load. This behavior can be attributed to the fact that higher inhomogeneity parameter k corresponds to lower volume fraction of the ceramic phase. However, the increases of the damping coefficient decrease critical buckling loads $\bar{N}$.

The buckling loads $\bar{N}$ of the (1–1–1) FGM sandwich square plate resting on Visco-Pasternak's elastic foundation with various boundary conditions for different values of damping coefficient are illustrated in Fig. 5 it is noted that $\bar{N}$ increase gradually as the side-to-thickness ratio a/h increases. The results of the simply-supported sandwich plate are less than that of the clamped–clamped and free–clamped sandwich plate. For the EGM sandwich plate with intermediate boundary conditions, the results take the corresponding intermediate values. Again, the increases of the damping coefficient increase critical buckling loads $\bar{N}$.

Fig. 6 shows the critical buckling loads $\bar{N}$ of the (1-1-1) FGM sandwich square plates under various boundary

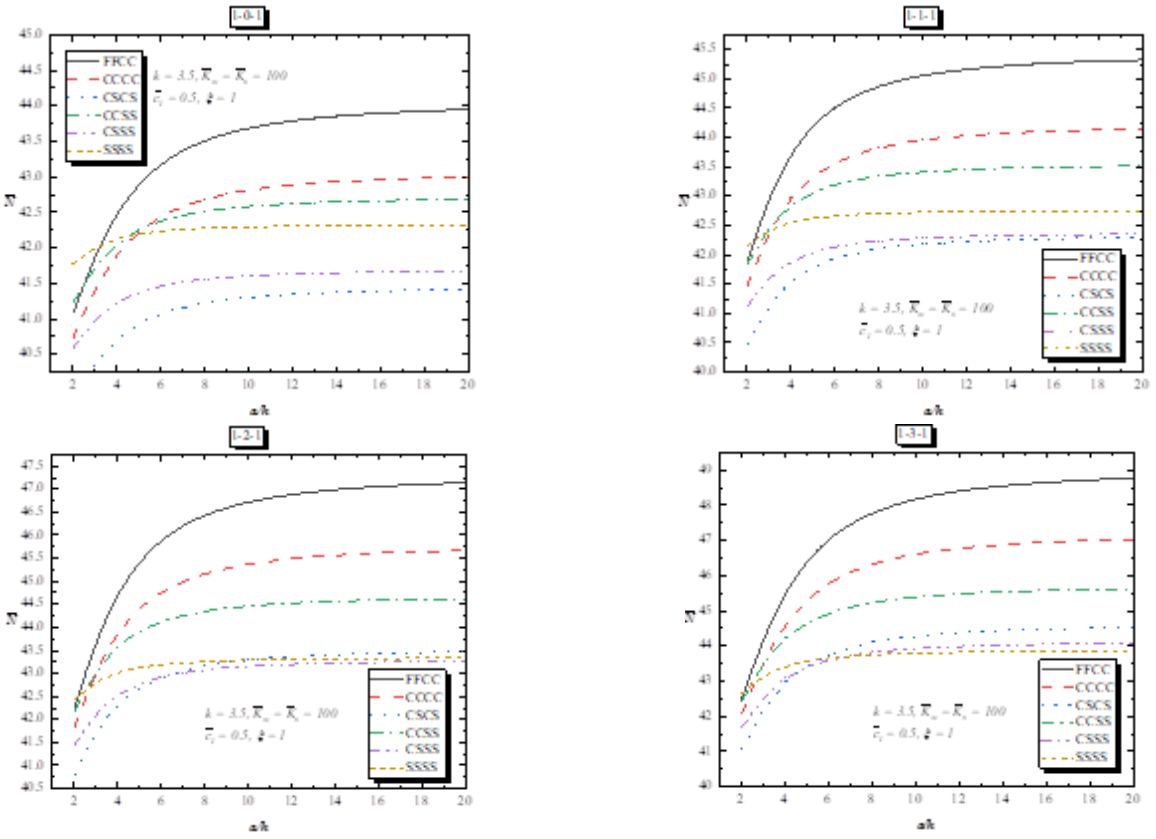

Fig. 7 Critical buckling load $\bar{N}$ versus the side-to-thickness ratio a/hand various types of FGM sandwich square plates resting on Visco-Pasternak's elastic foundation with various boundary conditions

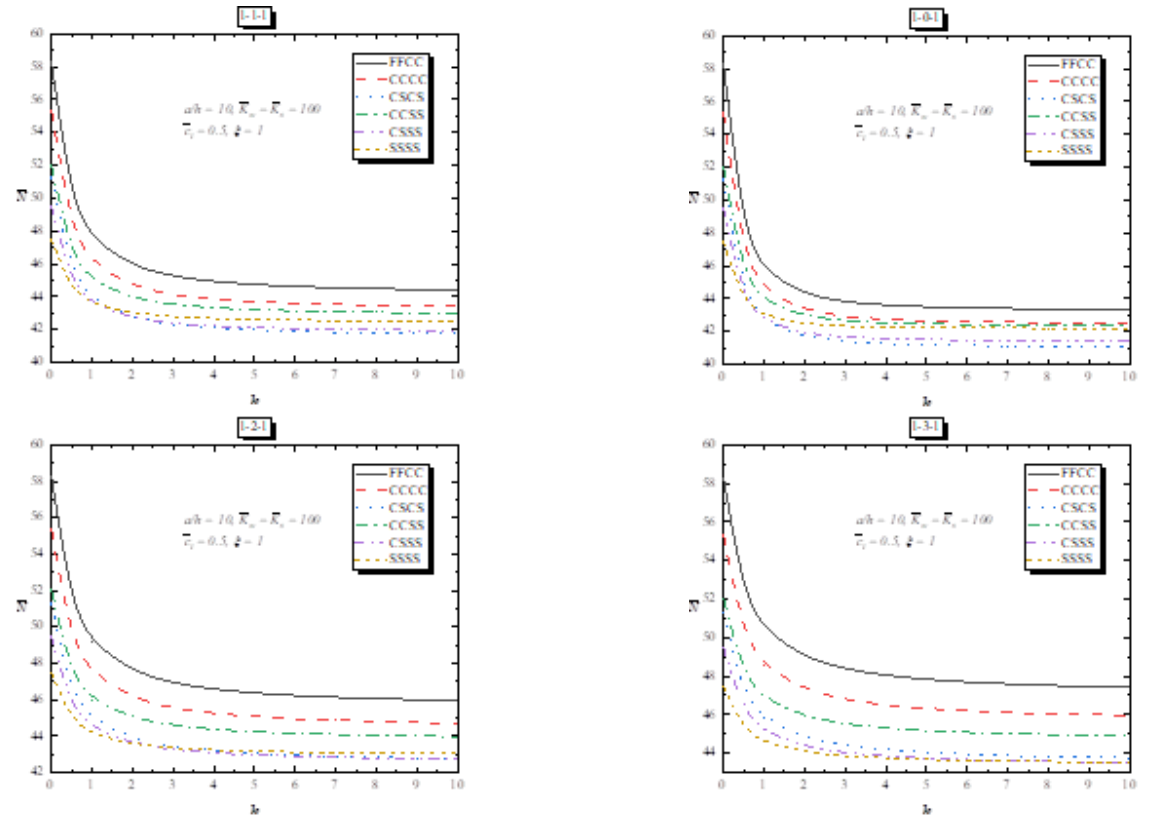

Fig. 8 Critical buckling $\bar{N}$ versus the gradient index k and various types of FGM sandwich square plates resting on Visco-Pasternak's elastic foundation with various boundary conditions

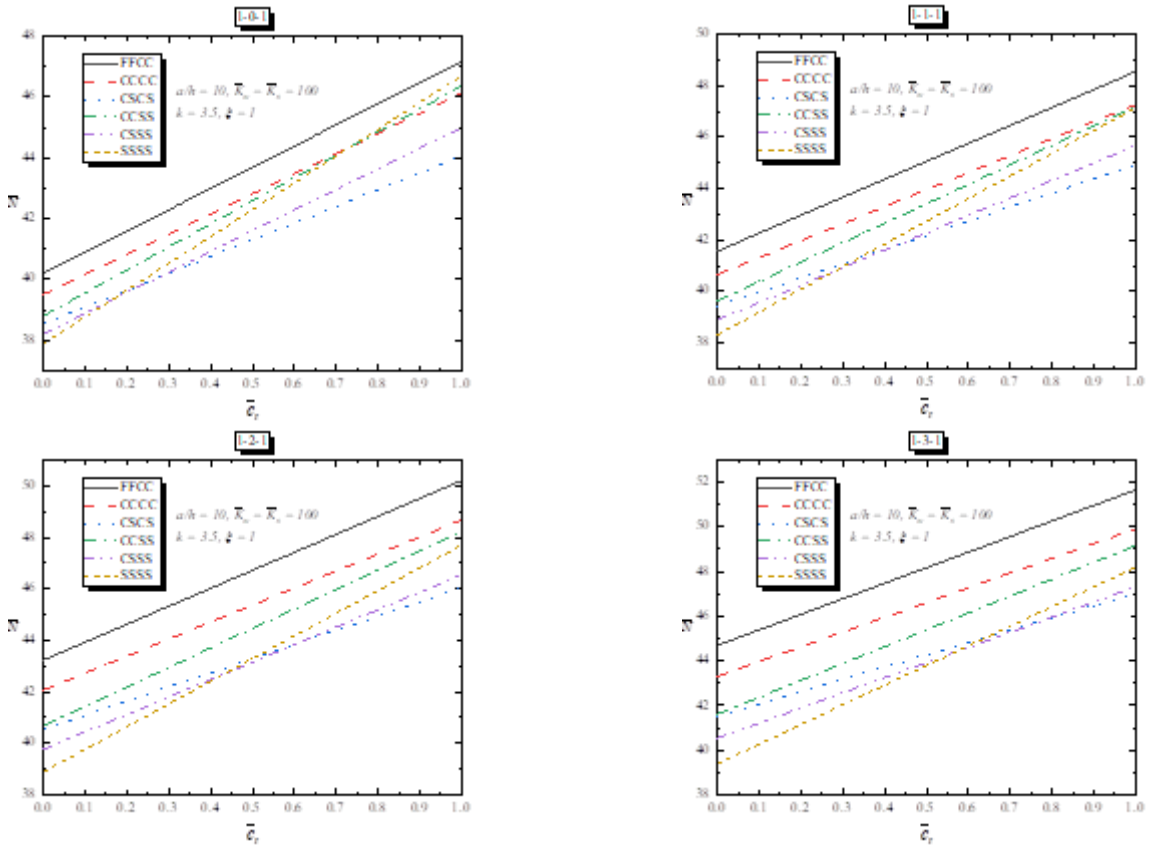

Fig. 9 Critical buckling $\bar{N}$ versus the damping coefficient and various types of FGM sandwich square plates resting on Visco-Pasternak's elastic foundation with various boundary conditions

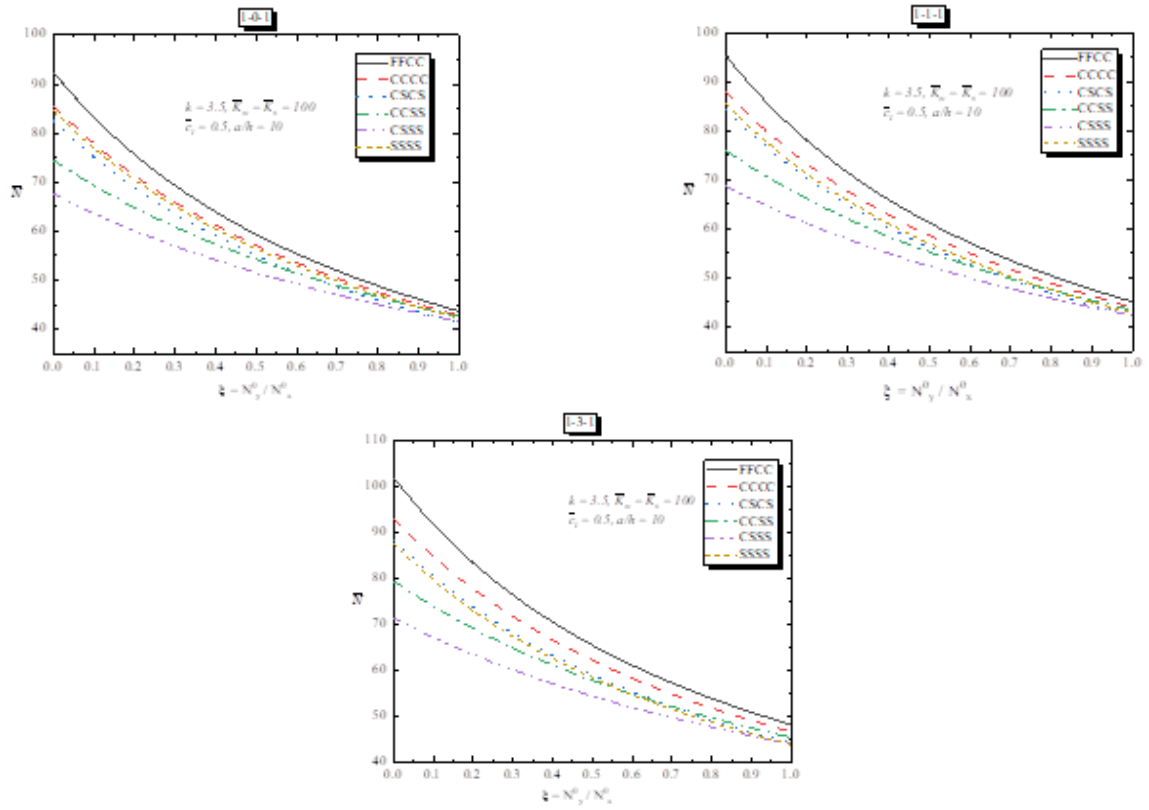

Fig. 10 Critical buckling $\bar{N}$ versus the different values of ξ and various types of FGM sandwich square plates resting on Visco-Pasternak's elastic foundation with various boundary conditions

conditions versus the damping coefficient c_t for different values of the inhomogeneity parameter k. It is observed that the increase of damping coefficient c_t leads to an increase of the critical buckling loads $\overline{N}$ of the FG sandwich plate.

Fig. 7 displays the critical buckling load $\overline{N}$ versus the side-to-thickness ratio a/h for different boundary conditions resting on visco-Pasternak foundation is presented. Different layer configurations are employed for multi-layered FGM plates. It can be seen that the critical buckling load $\overline{N}$ increases monotonically as a/h increases.

Fig. 8 presents the variation of the non-dimensional critical buckling loads $\overline{N}$ versus the gradient index k for diff erent values of damping coefficient. Different layer configurations are employed for multi-layered FGM plates with various boundary conditions. The thickness ratio of the plate is considered equal to 10. It can be observed that incre asing the inhomogeneity parameter k leads to a reduction of critical buckling load. This behavior can be attributed to the fact that higher inhomogeneity parameter k corresponds to l ower volume fraction of the ceramic phase.

Fig. 9 presents the variation of the non-dimensional critical buckling loads $\overline{N}$ versus the damping coefficient c_t of the various layer configurations for multi-layered FGM sandwich plates with various boundary conditions. The thickness ratio of the plate is considered equal to 10. It is observed that the increase of damping coefficient c_t leads to an increase of the critical buckling loads $\overline{N}$ of the FG sandwich plate.

Fig. 10 presents the variation of the non-dimensional critical buckling loads $\overline{N}$ for different values of ξ for various layer configurations for multi-layered FGM sandwich plates with various boundary conditions. The thickness ratio of the plate is considered equal to 10. It is observed that the increase of ξ leads to decrease the critical buckling loads $\overline{N}$ of the FG sandwich plate.

5. Conclusions

A simple trigonometric shear deformation model for buckling response of FG sandwich plates resting on visco-Pasternak foundations with different cases of boundary conditions is presented. The model contains only four unknown variables, satisfies the zero traction boundary conditions at the plate's surfaces without requiring a shear correction factor. The accuracy of the proposed formulation is proved by comparing it with existing solutions. The following conclusions may be drawn from the present analysis:

1. Excellent agreement was observed in all cases where the viscosity effect is omitted.
2. The inclusion of the viscosity effect makes a plate stiffer, and hence an increase of critical buckling loads $\overline{N}$.
3. The critical buckling load $\overline{N}$ are increasing with the increase of the parameters $\overline{K}_w$, $\overline{K}_s$ and $\overline{c}_t$.
4. A decrement for the critical buckling load can be clearly observed with the increase of the parameter k. The results of the simply-supported sandwich plate are less than that of the clamped-clamped and free-clamped sandwich plate.
5. The critical buckling load $\overline{N}$ increases monotonically as a/h increases.
6. The increase of $\xi = N_y^0/N_x^0$ leads to decrease the critical buckling loads $\overline{N}$.

References

Abdelrahman, W.G. (2020), "Effect of material transverse distribution profile on buckling of thick functionally graded material plates according to TSDT", *Struct. Eng. Mech*., **74**(1), 83-90. http://dx.doi.org/10.12989/sem.2020.74.1.083.

Adiyaman, G., Yaylaci, M. and Birinci, A. (2015), "Analytical and finite element solution of a receding contact problem", *Struct. Eng. Mech*., **54**(1), 69-85. https://doi.org/10.12989/sem.2015.54.1.069.

Ahmed, R.A., Fenjan, R.M. and Faleh, N.M. (2019), "Analyzing post-buckling behavior of continuously graded FG nanobeams with geometrical imperfections", *Geomech. Eng.*, **17**(2), 175-180. https://doi.org/10.12989/gae.2019.17.2.175.

Ait Amar Meziane, M., Abdelaziz, H.H. and Tounsi, A. (2014), "An efficient and simple refined theory for buckling and free vibration of exponentially graded sandwich plates under various boundary conditions", *J. Sandw. Struct. Mater*., **16**(3), 293-318. https://doi.org/10.1177/1099636214526852.

Akbas, S.D. (2015), "Wave propagation of a functionally graded beam in thermal environments", *Steel Compos. Struct.*, **19**(6), 1421-1447. https://doi.org/10.12989/SCS.2015.19.6.1421.

Akbaş, Ş.D. (2015), "Wave propagation of a functionally graded beam in thermal environments", *Steel Compos. Struct.*, **19**(6), 1421-1447. http://dx.doi.org/10.12989/scs.2015.19.6.1421.

Akgöz, B. and Civalek, Ö. (2013), "Buckling analysis of functionally graded microbeams based on the strain gradient theory", *Acta Mechanica*, **224**(9), 2185-2201. https://doi.org/10.1007/s00707-013-0883-5.

Allahkarami, F., Satouri, S. and Najafizadeh, M.M. (2016), "Mechanical buckling of two-dimensional functionally graded cylindrical shells surrounded by Winkler–Pasternak elastic foundation", *Mech. Adv. Mater. Struct*., **23**(8), 873-87. http://dx.doi.org/10.1080/15376494.2015.1036181.

Alnujaie, A., Akbas, Ş.D., Eltaher, M.A. and Assie, A. (2021), "Forced vibration of a functionally graded porous beam resting on viscoelastic foundation", *Geomech. Eng.*, **24**(1), 91-103. https://doi.org/10.12989/gae.2021.24.1.091.

Anderson, T.A. (2003), "A 3-D elasticity solution for a sandwich composite with functionally graded core subjected to transverse loading by a rigid sphere", *Compos. Struct.*, **60**(3), 265-274. https://doi.org/10.1016/s0263-8223(03)00013-8.

Arefi, M. and Zur, K.K. (2020), "Free vibration analysis of functionally graded cylindrical nanoshells resting on Pasternak foundation based on two-dimensional analysis", *Steel Compos. Struct.*, **34**(4), 615-623. https://doi.org/10.12989/scs.2020.34.4.615.

Asiri, S.A., Akbaş, Ş.D. and Eltaher, M.A. (2020), "Damped dynamic responses of a layered functionally graded thick beam under a pulse load", *Struct. Eng. Mech*., **75**(6), 713-722. https://doi.org/10.12989/sem.2020.75.6.713.

Attia, M.A. (2017), "On the mechanics of functionally graded nanobeams with the account of surface elasticity", *Int. J. Eng. Sci*., **115**, 73-101. https://doi.org/10.1016/j.ijengsci.2017.03.011.

Avcar, M. (2019), "Free vibration of imperfect sigmoid and power law functionally graded beams", *Steel Compos. Struct.*, **30**(6), 603-615. https://doi.org/10.12989/scs.2019.30.6.603.

Balubaid, M., Abdo, H., Ghandourah, E. and Mahmoud, S.R. (2021), "Dynamical behavior of the orthotropic elastic material using an analytical solution", *Geomech. Eng.*, **25**(4), 331-339. https://doi.org/10.12989/gae.2021.25.4.331.

Bashiri, A.H., Akbas, S.D., Abdelrahman, A.A., Assie, A., Eltaher, M.A. and Mohamed, E.F. (2021), "Vibration of multilayered functionally graded deep beams under thermal load", *Geomech. Eng.*, **24**(6), 545-557. https://doi.org/10.12989/gae.2021.24.6.545.

Bhangale, R.K. andGanesan, N. (2006), "Thermoelastic buckling and vibration behavior of a functionally graded sandwich beam with constrained viscoelastic core", *J. Sound Vib.*, **295**(1-2), 294-316. https://doi.org/10.1016/j.jsv.2006.01.026.

Bharath, H.S., Waddar, S., Bekinal, S.I., Jeyaraj, P. and Doddamani, M. (2020), "Effect of axial compression on dynamic response of concurrently printed sandwich", *Compos. Struct.*, 113223. https://doi.org/10.1016/j.compstruct.2020.113223.

Bouiadjra, R.B., Bachiri, A., Benyoucef, S., Fahsi, B. and Bernard, F. (2020), "An investigation of the thermodynamic effect on the response of FG beam on elastic foundation", *Struct. Eng. Mech*., **76**(1), 115-127. https://doi.org/10.12989/sem.2020.76.1.115.

Boulal, A., Bensattalah, T., Karas, A., Zidour, M., Heireche, H., and Adda Bedia, E.A. (2020), "Buckling of carbon nanotube reinforced composite plates supported by Kerr foundation using Hamilton's energy principle", *Struct. Eng. Mech.*, **73**(2), 209-223. https://doi.org/10.12989/sem.2020.73.2.209.

Chami, K, Messafer, T. and Hadji, L. (2020), "Analytical modeling of bending and free vibration of thick advanced composite beams resting on Winkler-Pasternak elastic foundation", *Earthq. Struct.*, **19**(2), 91-101. https://doi.org/10.12989/eas.2020.19.2.091.

Cuong-Le, T., Nguyen, K.D., Nguyen-Trong, N., Khatir, S., Nguyen-Xuan, H. and Abdel-Wahab, M. (2020a), "A three-dimensional solution for free vibration and buckling of annular plate, conical, cylinder and cylindrical shell of FG porous-cellular materials using IGA", *Compos. Struct*., **259**, 113216. https://doi.org/10.1016/j.compstruct.2020.113216.

Cuong-Le, T., Nguyen, K.D., Hoang-Le, M., Sang-To, T., Phan-Vu, P. and Abdel Wahab, M. (2022a), "Nonlocal strain gradient IGA numerical solution for static bending, free vibration and buckling of sigmoid FG sandwich nanoplate", *Physica B: Condensed Matter*, **631**, 413726. https://doi.org/10.1016/j.physb.2022.413726.

Cuong-Le, T., Nguyen, K.D., Lee, J., Rabczuk, T. and Nguyen-Xuan, H. (2022b), "A 3D nano scale IGA for free vibration and buckling analyses of multi-directional FGM nanoshells", *Nanotechnology*, **33**(6), 065703. https://doi.org/10.1088/1361-6528/ac32f9.

Cuong-Le, T., Nguyen, T.N., Vu, T.H., Khatir, S. and Abdel Wahab, M. (2020b), "A geometrically nonlinear size-dependent hypothesis for porous functionally graded micro-plate", *Eng. with Comput*., **38**(2022), 449-460. https://doi.org/10.1007/s00366-020-01154-0.

Daouadji, T.H. and Hadji, L. (2015), "Analytical solution of nonlinear cylindrical bending for functionally graded plates", *Geomech. Eng.*, **9**(5), 631-644. https://doi.org/10.12989/gae.2015.9.5.631.

Dehsaraji, M.L., Arefi, M. and Loghman, A. (2020), "Three dimensional free vibration analysis of functionally graded nano cylindrical shell considering thickness stretching effect", *Steel Compos. Struct.*, **34**(5), 657-670. https://doi.org/10.12989/scs.2020.34.5.657.

Ebrahimi, F. And Barati, M.R. (2016), "A nonlocal higher-order refined magneto-electro-viscoelastic beam model for dynamic analysis of smart nanostructures", *Int. J. Eng. Sci.*, **107**, 183-196. https://doi.org/10.1016/j.ijengsci.2016.08.001.

Ebrahimi, F. and Barati, M.R. (2016), "Vibration analysis of viscoelastic inhomogeneous nanobeams resting on a viscoelastic foundation based on nonlocal strain gradient theory incorporating surface and thermal effects", *Acta Mechanica*, **228**(3), 1197-1210. https://doi.org/10.1007/s00707-016-1755-6.

Eltaher, M.A. and Akbaş, Ş.D. (2020), "Transient response of 2D functionally graded beam structure", *Struct. Eng. Mech*., **75**(3), 357-367. https://doi.org/10.12989/SEM.2020.75.3.357.

Etemadi, E., AfaghiKhatibi, A. and Takaffoli, M. (2009), "3D finite element simulation of sandwich panels with a functionally graded core subjected to low velocity impact", *Compos. Struct*., **89**(1), 28-34. https://doi.org/10.1016/j.compstruct.2008.06.01.

Fan, Y., Xiang, Y. and Shen, H.S. (2018), "Nonlinear forced vibration of FG-GRC laminated plates resting on visco-Pasternak foundations", *Compos. Struct*., https://doi.org/10.1016/j.compstruct.2018.10.084.

Fan, Y., Xiang, Y., Shen, H.S. and Hui, D. (2018), "Nonlinear low-velocity impact response of FG-GRC laminated plates resting on visco-elastic foundations", *Compos. Part B: Eng.*, **144**, 184-194. https://doi.org/10.1016/j.compositesb.2018.02.016.

Feng, H., Shen, D. and Tahouneh, V. (2020), "Vibration analysis of sandwich sector plate with porous core and functionally graded wavy carbon nanotube-reinforced layers", *Steel Compos. Struct*. **37**(6), 711-731. http://dx.doi.org/10.12989/scs.2020.37.6.711.

Ghannadpour, S.A.M., Mohammadi, B. and Fazilati, J. (2013), "Bending, buckling and vibration problems of nonlocal Euler beams using Ritz method", *Compos. Struct*., **96**, 584-589. https://doi.org/ 10. 1016/j. compstruct. 2012. 08. 024.

Ghasemabadian, M.A. and Kadkhodayan, M. (2016), "Investigation of buckling behavior of functionally graded piezoelectric (FGP) rectangular plates under open and closed circuit conditions", *Struct. Eng. Mech.*, **60**(2), 271-299. https://doi.org/10.12989/sem.2016.60.2.271.

Hadji, L. (2020), "Influence of the distribution shape of porosity on the bending of FGM beam using a new higher order shear deformation model", *Smart Struct. Syst.*, **26**(2), 253-262. https://doi.org/10.12989/sss.2020.26.2.253.

Hadji, L. and Avcar, M. (2021), "Free vibration analysis of FG porous sandwich plates under various boundary conditions", *J. Appl. Comput. Mech.*, **7**(2) 505-519. https://doi.org/10.22055/JACM.2020.35328.2628.

Hosseini, M., Jamalpoor, A. and Bahreman, M. (2016), "Small-scale effects on the free vibrational behavior of embedded viscoelastic double-nanoplate-systems under thermal environment", *Acta Astronautica*, **129**, 400-409. https://doi.org/10.1016/j.actaastro.2016.10.001.

Hosseini, M., Jamalpoor, A. and Fath, A. (2016), "Surface effect on the biaxial buckling and free vibration of FGM nanoplate embedded in visco-Pasternak standard linear solid-type of foundation", *Meccanica*, **52**(6), 1381-1396. https://doi.org/10.1007/s11012-016-0469-0.

Huang, Z.Y., Lü, C.F. and Chen, W.Q. (2008), "Benchmark solutions for functionally graded thick plates resting on Winkler–Pasternak elastic foundations", *Compos. Struct.*, **85**(2), 95-104. https://doi.org/10.1016/j.compstruct.2007.10.010.

Karami, B. and Janghorban, M. (2020), "On the mechanics of functionally graded nanoshells", *Int. J. Eng. Sci*., **153**, 103309. https://doi.org/10.16/j.ijengsci.2020.103309

Katariya, P.V. and Panda, S.K. (2020), "Numerical analysis of thermal post-buckling strength of laminated skew sandwich composite shell panel structure including stretching effect", *Stee Compos. Struct*., **34**(2), 279-288. https://doi.org/10.12989/SCS.2020.34.2.279.

Kertész, S., Szerencsés, S.G., Veréb, G., Csanádi, J., László, Z., Hodúr, C. (2020), "Single- and multi-stage dairy wastewater treatment by vibratory membrane separation processes", *Membrane Water Treatment*, **11**(6), 383-389. https://doi.org/10.12989/mwt.2020.11.6.383.

Khatir, S., Tiachacht, S., Le Thanh, C., Ghandourah, E., Mirjalili, S. and Wahab, M.A. (2021), "An improved Artificial Neural Network using Arithmetic Optimization Algorithm for damage assessment in FGM composite plates", *Compos. Struct.*, **273**, 114287. https://doi.org/10.1016/j.compstruct.2021.114287.

Khatir, S., Tiachacht, S., Thanh, C.L., Bui, T.Q. and Wahab, M.A. (2019), "Damage assessment in composite laminates using ANN-PSO-IGA and Cornwell indicator", *Compos. Struct.*, **230**, 111509. https://doi.org/10.1016/j.compstruct.2019.111509

Kim, Y.W. (2015), "Free vibration analysis of FGM cylindrical shell partially resting on Pasternak elastic foundation with an oblique edge", *Compos. Part B: Eng.*, **70**, 263-276. https://doi.org/10.1016/j.compositesb.2014.11.024.

Koizumi, M. (1993), "The concept of FGM", *Ceramic Transactions, Functionally Gradient Materials.,* **34**, 3-10.

Kunbar, L.A.H., Hamad, L.B., Ahmed, R.A. and Faleh, N.M. (2020), "Nonlinear vibration of smart nonlocal magneto-electro-elastic beams resting on nonlinear elastic substrate with geometrical imperfection and various piezoelectric effects", *Smart Struct. Syst.*, **25**(5), 619-630. https://doi.org/10.12989/SSS.2020.25.5.619.

Li, J. and Zhang, Y. (2021), "Multiscale calculation results of the flow behavior in micro/nano porous filtration membrane with the adsorbed layer-fluid interfacial slippage", *Membrane Water Treatment*, **12**(3), 107-114. https://doi.org/10.12989/mwt.2021.12.3.107.

Li, M., GuedesSoares, C. and Yan, R. (2021), "Free vibration analysis of FGM plates on Winkler/Pasternak/Kerr foundation by using a simple quasi-3D HSDT", *Compos. Struct.*, **264**, 113643. https://doi.org/10.1016/j.compstruct.2021.113643.

Li, Z.M. and Yang, D.Q.(2016), "Thermal postbuckling analysis of anisotropic laminated beams with tubular cross-section based on higher-order theory", *Ocean Eng.*, **115**, 93-106. https://doi.org/10.1016/j.oceaneng.2016.02.017.

Madenci, E. (2019), "A refined functional and mixed formulation to static analyses of fgm beams", *Struct. Eng. Mech.*, **69**(4), 427-437. https://doi.org/10.12989/sem.2019.69.4.427.

Madenci, E. (2021), "Free vibration and static analyses of metal-ceramic FG beams via high-order variational MFEM", *Steel Compos. Struct.*, **39**(5), 493-509. https://doi.org/10.12989/scs.2021.39.5.493.

Mantari, J.L. and Granados, E.V. (2015a), "Dynamic analysis of functionally graded plates using a novel FSDT", *Compos. Part B: Eng.*, **75**, 148-155. https://doi.org/10.1016/j.compositesb.2015.01.028.

Mantari, J.L. and Granados, E.V. (2015b), "A refined FSDT for the static analysis of functionally graded sandwich plates", *Thin-Walled Struct.*, **90**, 150-158. https://doi.org/10.1016/j.tws.2015.01.015.

Merzoug, M., Bourada, M., Sekkal, M., Ali Chaibdra, A., Belmokhtar, C., Benyoucef, S. and Benachour, A. (2020), "2D and quasi 3D computational models for thermoelastic bending of FG beams on variable elastic foundation: Effect of the micromechanical models", *Geomech. Eng.*, **22**(4), 361-374. https://doi.org/10.12989/gae.2020.22.4.361.

Mindlin, R.D. (1951), "Thickness-shear and flexural vibrations of crystal plates", *J. Appl. Phys.*, **22**(3), 316-323. https://doi.org/10.1063/1.1699948.

Navale, K.U. and Pise, C.P. (2021), "A review on high order shear deformation theory for orthotropic composite laminates", *Int. J. Eng. Res. Technol.*, **10**, 477-481. https://doi.org/10.17577/IJERTV10IS010156.

Naz, A., Masood, H., Ehsan, S. and Tahir, T. (2020), "Removal of acid black 1 by Acacia Concinna; adsorption kinetics, isotherm and thermodynamic study", *Membrane Water Treatment*, **11**(6), 407-416. https://doi.org/10.12989/sem.2020.11.6.407.

Nebab, M., AitAtmane, H., Bennai, R. and Tahar, B. (2019), "Effect of nonlinear elastic foundations on dynamic behavior of FG plates using four-unknown plate theory", *Earthq. Struct.*, **17**(5), 447-462. https://doi.org/10.12989/eas.2019.17.5.447.

Nebab, M., Benguediab, S., AitAtmane, H and Bernard, F. (2020), "A simple quasi-3D HDST for dynamic behavior of advanced composite plates with the effect of variables elastic foundations", *Geomech. Eng.*, **22**(5), 415-431. https://doi.org/10.12989/gae.2020.22.5.415.

Neves, A.M.A., Ferreira, A.J.M., Carrera, E., Cinefra, M., Jorge, R.M.N. and Soares, C.M.M. (2012), "Buckling analysis of sandwich plates with functionally graded skins using a new quasi-3D hyperbolic sine shear deformation theory and collocation with radial basis functions", ZAMM – *J. Appl. Math. Mech. / Zeitschrift Für Angewandte Mathematik Und Mechanik*, **92**(9), 749-766. https://doi.org/10.1002/zamm.201100186.

Oner, E., Yaylaci, M. and Birinci, A. (2015), "Analytical solution of a contact problem and comparison with the results from FEM", *Struct. Eng. Mech.*, **54**(4), 607-622. https://doi.org/10.12989/sem.2015.54.4.607.

Onyeka, F.C. and Edozie, O. T. (2021), "Analytical solution of thick rectangular plate with clamped and free support boundary condition using polynomial shear deformation theory", *Adv. Sci. Technol. Eng. Syst. J.*, **6**(1), 1427-1439. https://doi.org/10.25046/aj0601161.

Panjehpour, M., Loh, E.W.K. and Deepak, TJ. (2018), "Structural Insulated Panels: State-of-the-Art", *Trends in civil Engineering and its Architecture*, **3**(1), 336-340. https://doi.org/10.32474/TCEIA.2018.03.000151.

Pasternak (1954), "On a new method of analysis of an elastic foundation by means of two foundation constants", *Gosudarstvennoe Izdatelstvo Literaturipo Stroitelstvui Arkhitekture*, Moscow.

Pasternak, P.L. (1954), "On a new method of analysis of an elastic foundation by means of two foundation constants", *Gosudarstvennoe Izdatelstro Liberaturipo Stroitelstvui Arkhitekture*, Moscow.

Rachedi, M.A., Benyoucef, S., Bouhadra, A., BachirBouiadjra, R., Sekkal, M. and Benachour, A. (2020), "Impact of the homogenization models on the thermoelastic response of FG plates on variable elastic foundation", *Geomech. Eng.*, **22**(1), 65-80. https://doi.org/10.12989/gae.2020.22.1.065.

Rahmani, M., Mohammadi, Y., Kakavand, F. and Raeisifard, H. (2020), "Vibration Analysis of Different Types of Porous FG Conical Sandwich Shells in Various Thermal Surroundings", *J. Appl. Comput. Mech.*, **6**(3), 416-432. https://doi.org/10.22055/jacm.2019.29442.1598.

Ramteke, P.M., Panda, S.K. and Sharma, N. (2019), "Effect of grading pattern and porosity on the eigen characteristics of porous functionally graded structure", *Steel Compos. Struct.*, **33**(6), 865-875. https://doi.org/10.12989/scs.2019.33.6.865.

Reissner, E. (1944), "On the theory of bending of elastic plates", *J. Math. Phys.*, **23**(1-4), 184-191. https://doi.org/10.1002/sapm1944231184.

Reissner, E. (1945), "The effect of transverse shear deformation on the bending of elastic plates", *J. Appl. Mech.*, **12**(2), 69-77. https://doi.org/10.1115/1.4009435.

Saadatmorad, M., Jafari-Talookolaei, R.A., Pashaei, M.H. and Khatir, S. (2021), "Damage detection on rectangular laminated composite plates using wavelet based convolutional neural network technique", *Compos. Struct.*, **278**, 114656. https://doi.org/10.1016/j.compstruct.2021.114656.

Sadoughifar, A., Farhatnia, F., Izadinia, M. and Talaeetaba, S.B. (2020), "Size-dependentbuckling behaviour of FG annular/circular thick nanoplates with porosities resting on Kerr foundation based on new hyperbolic shear deformation theory", *Struct. Eng. Mech.*, **73**(3), 225-238.

https://doi.org/10.12989/sem.2020.73.3.225.
Selmi, A. (2020), "Exact solution for nonlinear vibration of clamped-clamped functionally graded buckled beam", *Smart Struct. Syst.*, **26**(3), 361-371. https://doi.org/10.12989/sss.2020.26.3.361.
Shahmohammadi, M.A., Azhari, M. and Saadatpour, M.M. (2020), "Free vibration analysis of sandwich FGM shells using isogeometric B-spline finite strip method", *Steel Compos. Struct.*, **34**(3), 361-376. https://doi.org/10.12989/scs.2020.34.3.361.
Shen, H.S. and Yang, D.Q. (2014), "Nonlinear vibration of anisotropic laminated cylindrical shells with piezoelectric fiber reinforced composite actuators", *Ocean Eng.*, **80**, 36-49. https://doi.org/10.1016/j.oceaneng.2014.01.016.
Shodja, H., Haftbaradaran, H. and Asghari, M. (2007), "A thermoelasticity solution of sandwich structures with functionally graded coating", *Compos. Sci. Technol.*, **67**(6), 1073-1080. https://doi.org/10.1016/j.compscitech.2006.06.001.
Sobamowo, G. (2020), "Finite element thermal analysis of a moving porous fin with temperature-variant thermal conductivity and internal heat generation", *Reports in Mech. Eng.*, **1**(1), 110-127. https://doi.org/10.31181/rme200101110s.
Sobhy, M. (2013), "Buckling and free vibration of exponentially graded sandwich plates resting on elastic foundations under various boundary conditions", *Compos. Struct.*, **99**, 76-87. https://doi.org/10.1016/j.compstruct.2012.11.018.
Sobhy, M. and Zenkour, A.M. (2018), "Nonlocal thermal and mechanical buckling of nonlinear orthotropic viscoelastic nanoplates embedded in a visco-pasternak medium", *Int. J. Appl. Mech.*, **10**(8), 1850086. https://doi.org/10.1142/S1758825118500862.
Timesli, A. (2020), "Prediction of the critical buckling load of SWCNT reinforced concrete cylindrical shell embedded in an elastic foundation", *Comput. Concrete.*, **26**(1), 53-62. https://doi.org/10.12989/cac.2020.26.1.053.
Tj, H.G., Mikami, T., Kanie, S. andSato, M. (2006), "Free vibration characteristics of cylindrical shells partially buried in elastic foundations", *J. Sound Vib.*, **290**(3-5), 785-793. https://doi.org/10.1016/j.jsv.2005.04.014.
Tornabene, F., Fantuzzi, N., Viola, E. and Reddy, J.N. (2014), "Winkler–Pasternak foundation effect on the static and dynamic analyses of laminated doubly-curved and degenerate shells and panels", *Compos. Part B: Eng.*, **57**, 269-296. https://doi.org/10.1016/j.compositesb.2013.06.020.
Trabelsi, S., Zghal, S. and Dammak, F. (2020), "Thermo-elastic buckling and post-buckling analysis of functionally graded thin plate and shell structures", *J. Brazilian Soc. Mech. Sci. Eng.*, **42**(5), 1-22. https://doi.org/10.1007/s40430-020-02314-5.
Tran, T.M. and Cuong-Le, T. (2022), "A nonlocal IGA numerical solution for free vibration and buckling analysis of porous sigmoid functionally graded (P-SFGM) nanoplate", *Int. J. Struct. Stab. Dyn.*, **22**(16), 2250193. https://doi.org/10.1142/S0219455422501930.
Vinh, P.V. (2021), "Formulation of a new mixed four-node quadrilateral element for static bending analysis of variable thickness functionally graded material plates", *Math. Probl. Eng.*, **2021**, 23. https://doi.org/10.1155/2021/6653350.
Vinyas, M. (2020), "On frequency response of porous functionally graded magneto-electro-elastic circular and annular plates with different electro-magnetic conditions using HSDT", *Compos. Struct.*, 240, 112044. https://doi.org/10.1016/j.compstruct.2020.112044.
Wang, Y.Q. and Zu, J.W. (2017), "Vibration behaviors of functionally graded rectangular plates with porosities and moving in thermal environment", *Aerosp. Sci. Technol.*, **69**, 550-562. https://doi.org/10.1016/j.ast.2017.07.023.
Wang, Y.Q., Huang, X.B. and Li, J. (2016), "Hydroelastic dynamic analysis of axially moving plates in continuous hot-dip galvanizing process", *Int. J. Mech. Sci.*, **110**, 201-216. https://doi.org/10.1016/j.ijmecsci.2016.03.010.
Wang, Z.X. andShen, H.-S. (2013), "Nonlinear dynamic response of sandwich plates with FGM face sheets resting on elastic foundations in thermal environments", *Ocean Eng.*, **57**, 99-110. https://doi.org/10.1016/j.oceaneng.2012.09.004.
Winkler, E. (1867), "Die Lehre von Elastizitat und Festigkeit (on ElasticityandFixity)", *Dominicus*, Prague.
Yaghoobi, H. and Yaghoobi, P. (2013), "Buckling analysis of sandwich plates with FGM face sheets resting on elastic foundation with various boundary conditions: an analytical approach", *Meccanica*, **48**(8), 2019-2035. https://doi.org/10.1007/s11012-013-9720-0.
Yamanoushi, M., Koizumi, M., Hiraii, T. and Shiota, I. (1990), "Proceedings of the first international symposium on functionally gradient materials", Japan.
Yaylacı, E.U., Yaylacı, M., Ölmez, H. and Birinci, A. (2020a), "Artificial neural network calculations for a receding contact problem", *Comput. Concrete*, **25**(6), 551-563. https://doi.org/10.12989/cac.2020.25.6.551.
Yaylacı, M. (2016), "The investigation crack problem through numerical analysis", *Structural Engineering and Mechanics, An Int'l Journal*, **57**(6), 1143-1156. https://doi.org/10.12989/sem.2016.57.6.1143
Yaylaci, M. and Birinci, A. (2013), "The receding contact problem of two elastic layers supported by two elastic quarter planes", *Struct. Eng. Mech.*, **48**(2), 241-255. https://doi.org/10.12989/sem.2013.48.2.241.
Yaylaci, M., Adiyaman, G., Oner, E. and Birinci, A. (2020b), "Examination of analytical and finite element solutions regarding contact of a functionally graded layer", *Struct. Eng. Mech.*, **76**(3), 325-336. https://doi.org/10.12989/sem.2020.76.3.325.
Yaylaci, M., Adiyaman, G., Oner, E. and Birinci, A. (2021c), "Investigation of continuous and discontinuous contact cases in the contact mechanics of graded materials using analytical method and FEM", *Comput. Concrete*, **27**(3), 199-210. https://doi.org/10.12989/cac.2021.27.3.199.
Yaylacı, M., Eyüboğlu, A., Adıyaman, G., Yaylacı, E.U., Öner, E. and Birinci, A. (2021a), "Assessment of different solution methods for receding contact problems in functionally graded layered mediums", *Mech. Mater.*, **154**, 103730. https://doi.org/10.1016/j.mechmat.2020.103730.
Yaylaci, M., Yayli, M., Yaylaci, E.U., Olmez, H. and Birinci, A. (2021d), "Analyzing the contact problem of a functionally graded layer resting on an elastic half plane with theory of elasticity, finite element method and multilayer perceptron", *Struct. Eng. Mech.*, **78**(5), 585-597. https://doi.org/10.12989/sem.2021.78.5.585.
Zamani, H.A., Aghdam, M.M. and Sadighi, M. (2017), "Free vibration analysis of thick viscoelastic composite plates on visco-Pasternak foundation using higher-order theory", *Compos. Struct.*, **182**, 25-35. https://doi.org/10.1016/j.compstruct.2017.08.101.
Zamani, H.A., Aghdam, M.M. and Sadighi, M. (2017), "Free vibration analysis of thick viscoelastic composite plates on visco-Pasternak foundation using higher-order theory", *Compos. Struct.*, **182**, 25-35. https://doi.org/10.1016/j.compstruct.2017.08.101.
Zenkour, A.M. (2018), "A quasi-3D refined theory for functionally graded single-layered and sandwich plates with porosities", *Compos. Struct.*, **201**, 38-48. https://doi.org/10.1016/j.compstruct.2018.05.147.
Zenzen, R., Khatir, S., Belaidi, I., Le Thanh, C. and Wahab, M.A. (2020), "A modified transmissibility indicator and Artificial Neural Network for damage identification and quantification in

laminated composite structures", *Compos. Struct.*, **248**, 112497. https://doi.org/10.1016/j.compstruct.2020.112497.

Zhang, W. (2001), "Global and chaotic dynamics for a parametrically excited thin plate", *J. Sound Vib.*, **239**(5), 1013-1036. https://doi.org/10.1006/jsvi.2000.3182.

Zouatnia, N. and Hadji, L. (2019), "Static and free vibration behavior of functionally graded sandwich plates using a simple higher order shear deformation theory", *Adv. Mater. Res*., **8**(4), 313-335. https://doi.org/10.12989/amr.2019.8.4.313.

CC